

OPTIMIZATION OF CROSS FLOW FAN HOUSING
FOR AIRPLANE WING INSTALLATION

APPROVED:

Donald R. Wilson

(Supervising Professor)

D D Seath

J. Fairchild

S. R. Benfield

OPTIMIZATION OF CROSS FLOW FAN HOUSING
FOR AIRPLANE WING INSTALLATION

by

KALPANA CHAWLA

Presented to the Faculty of the Graduate School of
The University of Texas at Arlington in Partial Fulfillment
of the Requirements
for the Degree of

MASTER OF SCIENCE IN AEROSPACE ENGINEERING

THE UNIVERSITY OF TEXAS AT ARLINGTON

July 1984

ACKNOWLEDGMENTS

I wish to express my deep gratitude to my parents for having funded my educational expenses enabling me to earn my Master's Degree. I wish to thank Dr. Donald R. Wilson of the Aerospace Engineering Department for his invaluable support and encouragement during both the experimental and theoretical stages of my research. I would also like to thank Jim Holland of the Aerospace Engineering Lab for his technical assistance during the experimental stages of my research. I would like to thank J. P. Harrison for his unceasing encouragement during my attendance at U.T.A.

April 16, 1984

ABSTRACT

OPTIMIZATION OF CROSS FLOW FAN HOUSING
FOR AIRPLANE WING INSTALLATION

Kalpana Chawla, M.S.

The University of Texas at Arlington, 1984

Supervising Professor: Donald R. Wilson

The research dealt primarily with the optimization of the cross flow fan housing for its installation in an airplane wing.

A cross flow fan was installed in a NACA 0018 wing section and various housing shapes were tested until a housing shape was obtained that trapped both the primary and secondary vortices, so that maximum throughput could be obtained. For this wing section, data was collected and the pressure coefficient distribution on upper surface was

obtained. There was a significant rise in the absolute magnitude of pressure coefficient distribution on the upper surface with the fan running. Momentum coefficient values as high as 1 were obtained, which implied that such an arrangement could be used in an airplane to improve its STOL capability.

TABLE OF CONTENTS

ACKNOWLEDGMENTS	iii
ABSTRACT	iv
LIST OF FIGURES	viii
LIST OF SYMBOLS	xii
CHAPTER 1 INTRODUCTION	1
1.1 Definitions	2
1.2 The historical problem	4
CHAPTER 2 HYDRAULIC ANALOGY	16
CHAPTER 3 CONTROL VOLUME ANALYSIS	20
3.1 Integral equations	20
3.2 The ideal velocity triangle analysis	21
CHAPTER 4 FAN DESIGN	29
4.1 Radius ratio	29
4.2 Solidity	30
4.3 Blade discharge angle	31
4.4 Cavity design	32
4.5 Dimensional Analysis	33
CHAPTER 5 EXPERIMENTAL PROGRAM	41
5.1 Sources of error	41
5.2 First design	42
5.3 Housing	43
5.4 First modification	44

5.5	Second modification	46
5.6	Third modification	46
5.7	Low R.P.M. experiment	47
5.8	Inlet modification and chord reduction	48
5.9	Smaller fan experiment	49
CONCLUSION	94
REFERENCES	96

LIST OF FIGURES

1.1	C.F.F. Installation in a wing	8
1.2	Schematic of a C.F.F.	9
1.3	Primary vortex sealing the return flow	10
1.4	Eck's C.F.F. design.....	11
1.5	C.F.F. with log spiral wall	12
1.6	C.F.F performance as a function of baffle design .	13
1.7	Best angular placing of the inlet, low pressure cavity, outlet and high pressure cavity	14
1.8	Traditional and simple design of C.F.F. secondary cavity exhibit same performance	15
2.1	Notation for hydraulic analogy equations	19
3.1	Control volume for a C.F.F.	24
3.2	Stations for velocity triangle analysis	25
3.3	Ideal analysis of velocity triangles	26
3.4	Higher incoming absolute velocity requires an increase in blade speed	27
3.5	Lower incoming absolute velocity requires a decrease in blade speed	28
4.1	Fan variables	35
4.2	Effect of vortex center location on flow coefficient	36

4.3	Effect of vortex center location on pressure coefficient	37
4.4	Effect of impeller radius ratio on pressure coefficient	38
4.5	Longer chord resulting in accentuation of nozzle action	39
4.6	Direction of vortices for a good through flow	40
5.1	Experimental setup in the water table	51
5.2	Airfoil dividing water table into diffuser and nozzle	52
5.3	First design, fan installation at maximum thickness	53
5.4	First design with elliptical cavity and return flow at the inlet	54
5.5	First design at a nose dip placing	55
5.6	Higher momentum coefficient leading to higher lift coefficient at same angles of attack	56
5.7	Best angular placing of the inlet, low pressure cavity, outlet and high pressure cavity	57
5.8	New inlet and exit design	58
5.9	First design at $\alpha = 0$	59
5.10	Configuration of fig. 5.9 with closed inlet	60
5.11	First airfoil at angle of attack with dip nose ...	61
5.12	First airfoil at angle of attack	62
5.13	Second modification, shallower primary cavity	63
5.14	Third modification, deeper primary cavity	64

5.15	Deeper primary cavity in airfoil	65
5.16	Configuration of fig. 5.15 with closed inlet	66
5.17	Forcing primary vortex to move in right direction	67
5.18	Fourth modification, partial flow obstruction to primary cavity	68
5.19	Low R.P.M. experiment	69
5.20	Low R.P.M. experiment with airfoil at an angle of attack	70
5.21	Configuration of fig. 5.20 with fan off	71
5.22	Modified inlet and chord	72
5.23	Modified inlet with rear airfoil shaped so that flow can be picked up from rear also	73
5.24	Theoretical streamline pattern through a C.F.F. ..	74
5.25	Modified inlet airfoil at low R.P.M.	75
5.26	Modified inlet airfoil with fan off at low A.O.A..	76
5.27	Configuration of figure 5.26 with fan running	77
5.28	Modified inlet airfoil with fan off at high A.O.A.	78
5.29	Configuration of figure 5.28 with fan running	79
5.30	Pressure coefficient distribution on the upper surface along chord at $\alpha = 12^\circ$ (Big fan).....	80
5.31	Pressure coefficient distribution on the upper surface along chord at $\alpha = 13.6^\circ$ (Big fan)	81
5.32	Pressure coefficient distribution on the upper surface along chord at $\alpha = 27^\circ$ (Big fan)	82

5.33	Momentum coefficient as a function of A.O.A.	83
5.34	Small fan dimensions	84
5.35	Small fan experiment in the setup of modified inlet	85
5.36	Location of centers of primary and secondary vortices	86
5.37	Vortex location with and without casing	87
5.38	Airfoil with modified inlet and small fan at A.O.A	88
5.39	Configuration of figure 5.38 with fan running	89
5.40	Pressure coefficient distribution on the upper surface along chord at $\alpha = 3.8^\circ$ (Small fan)	90
5.41	Pressure coefficient distribution on the upper surface along chord at $\alpha = 8.3^\circ$ (Small fan)	91
5.42	Pressure coefficient distribution on the upper surface along chord at $\alpha = 12^\circ$ (Small fan)	92
5.43	Pressure coefficient distribution on the upper surface along chord at $\alpha = 31.4^\circ$ (Small fan)	93

LIST OF SYMBOLS

a	sonic velocity, vortex center radius ratio.
A	area
A.O.A	angle of attack
bHP	brake horse power
c	fan blade chord
C	absolute velocity
C.F.F	Cross Flow Fan
C_h	head coefficient
C_l	lift coefficient
C_μ	momentum coefficient
C_p	power coefficient, pressure coefficient
d	depth of water surface at point of concern
d_o	depth of water surface at originating point.
D	fan diameter
D_h	hydraulic diameter
F	Froude number
g	acceleration due to gravity
H	pressure head
HP	horse power
L	fan span
L/S	lower surface
M	Mach number
n	unit vector perpendicular to elemental area dA
N	fan R.P.M.

p	static pressure
p_0	total pressure,
Q	volume flow rate
q	dynamic pressure
r	radius
S	surface area
t	static temprature
T_0	total temprature
U	blade speed
U/S	upper surface
V	water velocity
V	jet velocity
V	free stream velocity
W	relative velocity
z	height of flow filament above tank bottom
z_0	height of flow filament above tank bottom at originating point.

GREEK SYMBOLS

μ	viscosity
ϕ	flow coefficient
ψ	pressure coefficient
ρ	density
η	hydraulic efficiency
τ	torque
β_0	blade discharge angle (angle between tangent to blade at outer tip and line joining fan center to the outer tip)
β_2	blade discharge angle ($90 - \beta_0$)
θ	angular displacement of vortex from horizontal axis
θ	angular displacement from horizontal axis
α	angle of attack

SUBSCRIPTS

1	outer
2	inner
d	discharge
i	inner
o	outer
s	suction
tip	at tip
θ	tangential

CHAPTER 1

INTRODUCTION

Cross Flow Fans (C.F.F.) have been used for various reasons in the past, such as: 1) mine ventilation, 2) grain drying and 3) blowers for hair dryers. Active investigation is also in progress for application to Gas Dynamic lasers.

In 1962, Dornier proposed the installation of such a fan in a wing as shown in fig.1.1. Since then the idea of using a C.F.F. in an airplane wing has been picked up and discarded over and over again because of the extremely low order of efficiency (about 50%) that these fans had exhibited. However, work done in the 70's brought the efficiency of the C.F.F. above 80%. Such a fan would have the potential for improving the STOL capability of an airplane.

The present research is addressed to the problem of design of the housing of such a fan for installation in an airplane wing. Benefits derived from such an installation would be primarily:

- 1) Boundary layer control by boundary layer suction. Flow would be picked up from the lower surface and injected on the upper surface. Compared to conventional schemes of controlling boundary layers such as: blown flaps,

slots, blown wing and vortex generators, this system would accelerate the incoming flow and exhaust it over the upper surface, creating both extra lift and thrust along with boundary layer control. Extra lift would result because of the flow acceleration on the upper surface resulting in higher dynamic pressure. Extra thrust would result because of the jet velocity exhausted over the upper surface being greater than the incoming flow velocity.

- 2) Improvement in the STOL capability of an airplane.
- 3) Thrust vectoring.

A C.F.F. operates by transversally accelerating the flow picked up at an inlet and exhausted through an outlet. Compared to an axial fan, where the flow is axial and hence essentially one dimensional in nature, in a C.F.F. the flow is transverse and hence two dimensional in nature. Because of its two dimensional nature, the C.F.F. could be installed very easily along a wing span. A C.F.F. schematic is shown in fig. 1.2.

1.1 Definitions

The following definitions have been used by different researchers to determine the characteristics of a C.F.F. (ref.1):

Flow Coefficient:

$$\phi = \frac{Q}{L D U_{\text{tip}}} \quad 1.1$$

For airplane applications, the flow coefficient should be as high as possible, because this implies more mass flux and hence more momentum flux.

Pressure Coefficient:

$$\psi = \frac{\Delta P_o}{1/2 \rho U_{\text{tip}}^2} \quad 1.2$$

For airplane applications, the total pressure coefficient should also be as high as possible as this implies an increase in airflow velocity as the flow passes through the C.F.F. and over the upper wing surface.

Certain researchers have thought of using the C.F.F. to obtain a high static pressure coefficient. Since in the present research, the flow is picked up from the lower wing surface and discharged on the upper wing surface, a high static pressure coefficient would be undesirable.

Efficiency:

$$\eta = \frac{Q \Delta P_o}{\text{Input shaft H.P}}$$

For any application, a mechanical device should have a high efficiency, especially in an airplane where weight is of critical concern.

1.2 The Historical Problem

When a Cross Flow Fan rotates, it generates a large internal vortex system. Because of the presence of this vortex system, through flow cannot be obtained efficiently, without a proper C.F.F. housing design.

In the past, most researchers have addressed the problem of the housing design for the C.F.F. installed in mechanical devices with no air interaction at inlet and outlet. Very few researchers have dealt with the problem of a C.F.F. installed in the wing where the flow at the inlet and outlet is dynamic.

Researchers have worked on the C.F.F. since the late 19th century. In 1890, P. Mortier designed the first C.F.F. with a solid shaft and a solid body. Schmarje in 1910, Dalin in 1929, Sprenger in 1937, Eck in early 1950's and Coester,

Englehardt, Ilberg and Sadeh, Porter and Markland, J. P. Hancock and Gary Harloff in the second half of 20th century have worked on the design of the C.F.F. An excellent review of the literature can be found in ref. 1.

The researchers have tried to partially capture the central vortex in a cavity and using this vortex to seal the return flow as shown in fig.1.3. They have tried to improve the pressure coefficient, the flow coefficient and C.F.F. efficiency by trying to find the various parameters that influence fan performance.

A. M. Porter and E. Markland (ref.2), in their research done in the 1970's, showed that by proper design the vortex can be made to remain close to the rotor periphery over the full operating range. They also showed that the design of the outer wall or the secondary cavity is very important to the vortex position and that pressure recovery is not dependent upon an effective diffusing outlet section as had been thought. They compared performance of fans designed by other researchers, and used Eck's design (fig.1.4) as the starting design. The various changes in the wall design led them to the log spiral wall (fig.1.5) with which they obtained very good performance.

Ilberg and Sadeh (ref.3), in 1965, did testing of Cross Flow Fans and observed that the fan performance is very sensitive to the diffuser baffle, as shown in fig.1.6.

They stated that the system efficiency increases with an increase in impeller speed although they were not able to show this experimentally, as the speed of their fan could not be increased beyond 2500 R.P.M due to mechanical reasons. They found that the flow regime through the fan could be controlled and that the location of the vortex depended on the diffuser baffle. They also observed a secondary flow perpendicular to the primary flow.

Harloff (ref.1) in 1979, based on his experimental research found that the following parameters influenced the fan performance most, in decreasing order of importance:

Exit height

Low pressure cavity shape

Inlet arc

Exit housing shape

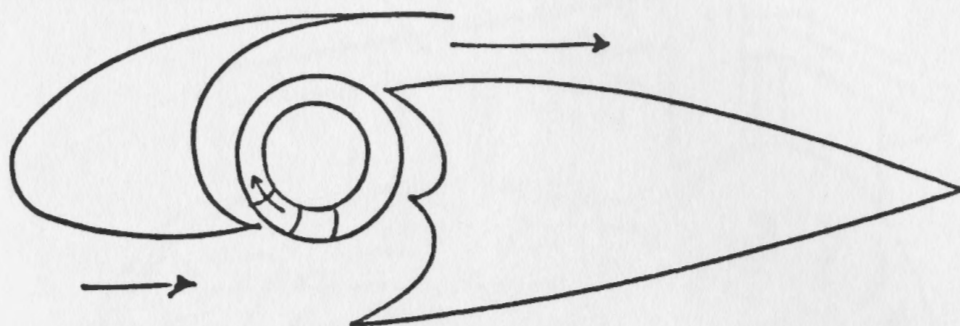
Fan blade design

He came up with best angular placings of the inlet, high pressure cavity, outlet and the low pressure cavity (fig.1.7). For the first time, the C.F.F. experimental analysis was taken to the transonic regime.

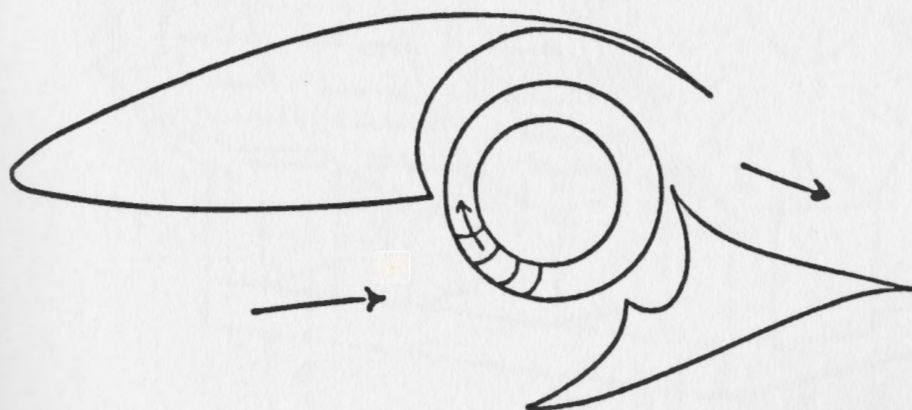
J. P. Hancock (ref.4), in his research published in 1980 found that maximum efficiency could be obtained by having a large region of recirculating flow inside the fan. With a large amount of flow recirculating inside the fan,

the flow coefficient was reduced substantially. He stated that for his final design (fig.1.8), the size of the secondary cavity did not influence the fan performance.

From the survey of this literature, it has been found that the primary vortex must be positioned to preclude any return flow at the inlet. Vortex positioning is dependent upon the housing design. High values of the flow and pressure coefficients can be obtained by positioning this vortex in a housing or a cavity. Shallow cavities may result in lesser through flow because of vortex occupying most of the place at the outlet region. Variables that affect the flow and pressure coefficients values most are: Housing design, inlet arc, exit height, fan geometry and fan speed.



Forward Installation



Aft Installation

Figure 1.1 C.F.F. installation in a wing. (Ref. 1)

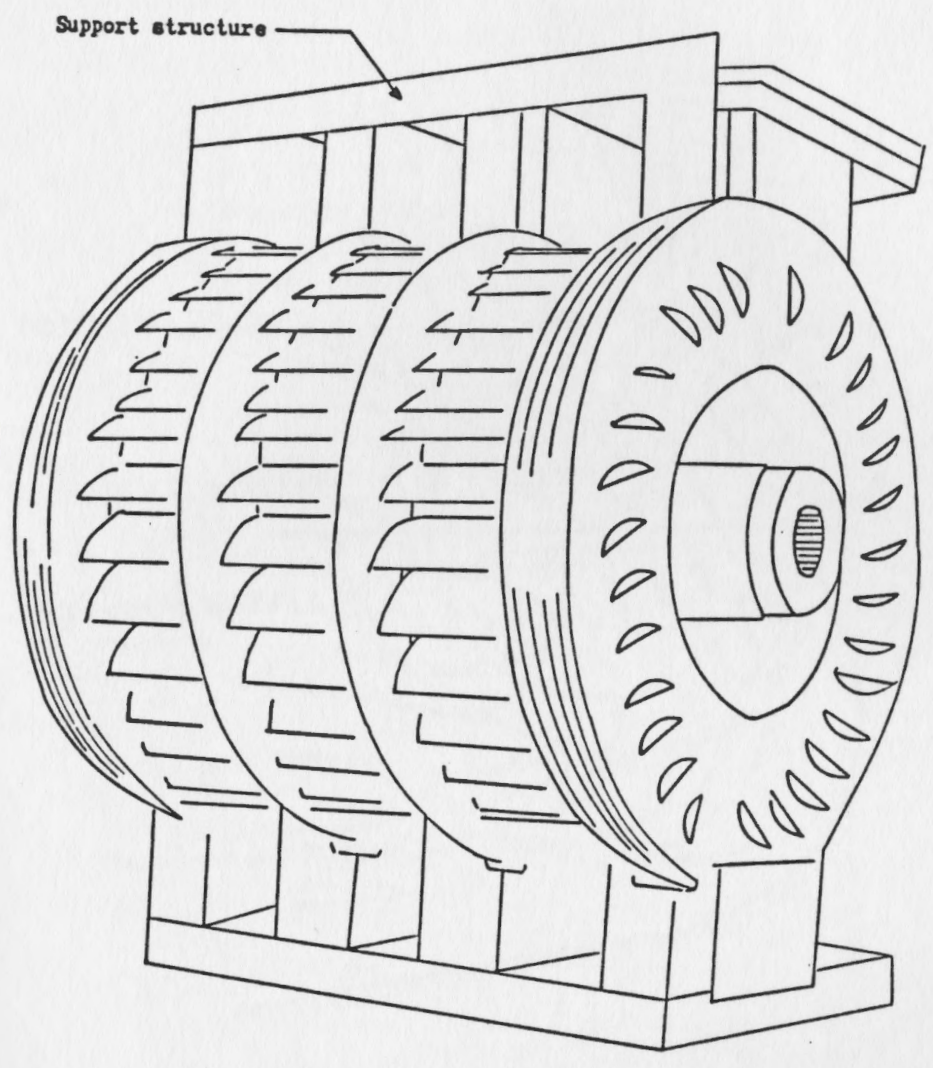


Figure 1.2 Schematic of a C.F.F (Ref. 1)

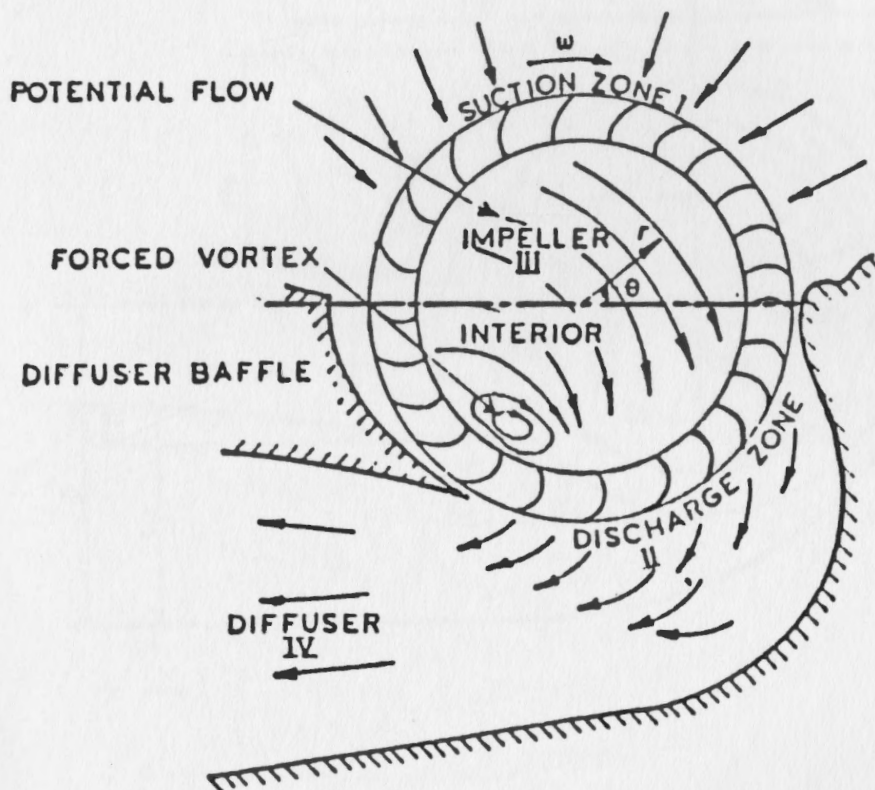


Figure 1.3 Primary vortex sealing the return flow. (Ref. 3)

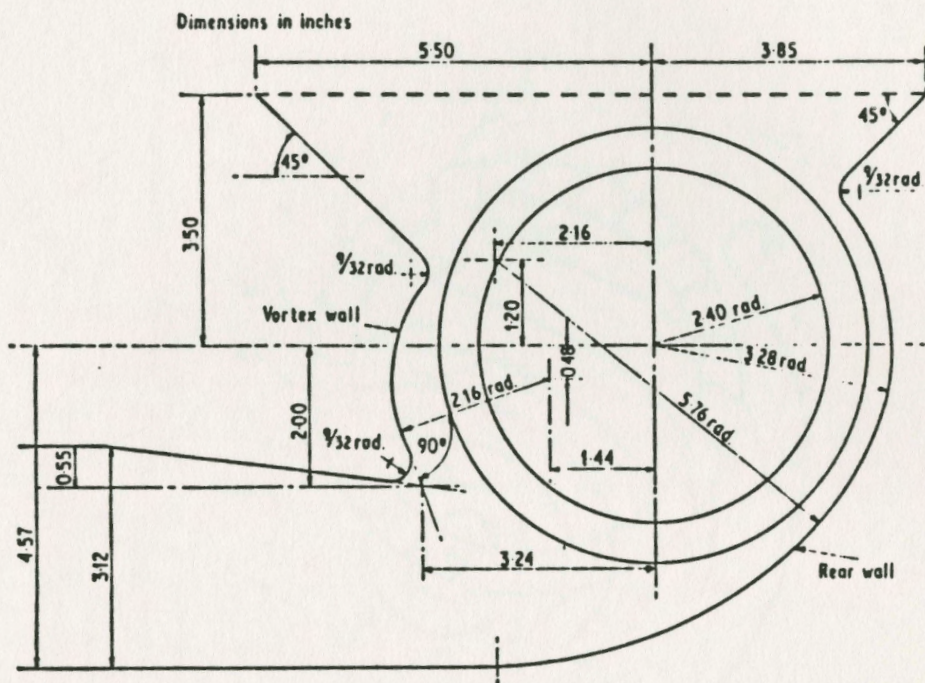


Figure 1.4 Eck's Cross Flow Fan Design. (Ref. 2)

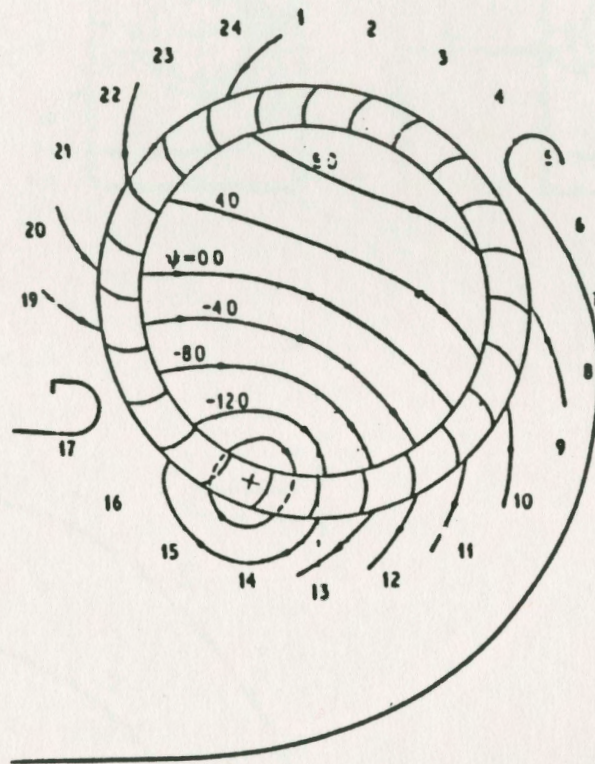


Figure 1.5 Cross Flow Fan with log spiral wall. (Ref. 2)

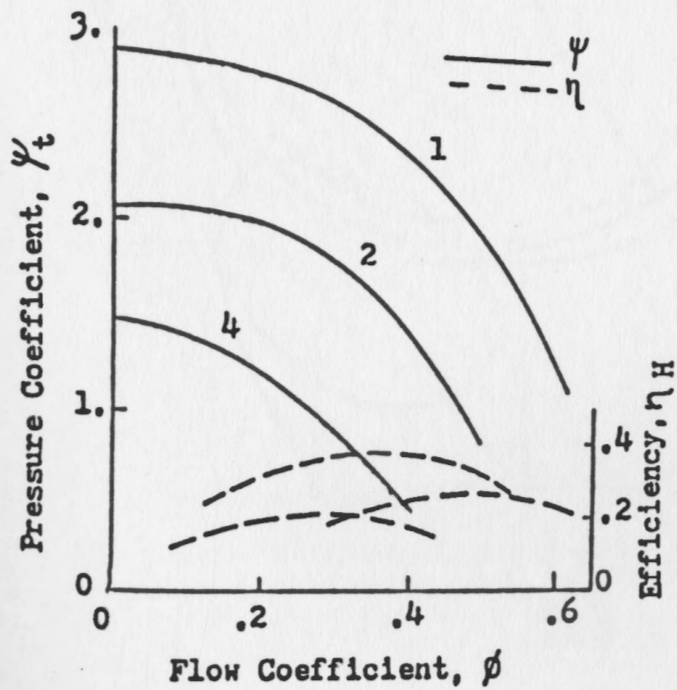
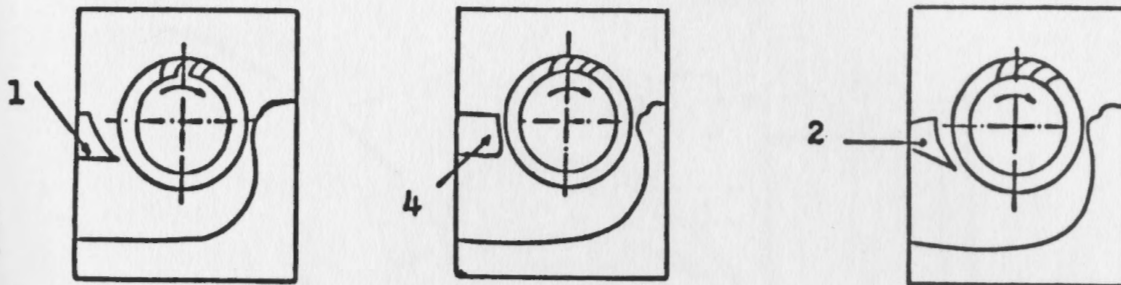


Figure 1.6 C.F.F performance as a function of baffle design. (Ref. 1)

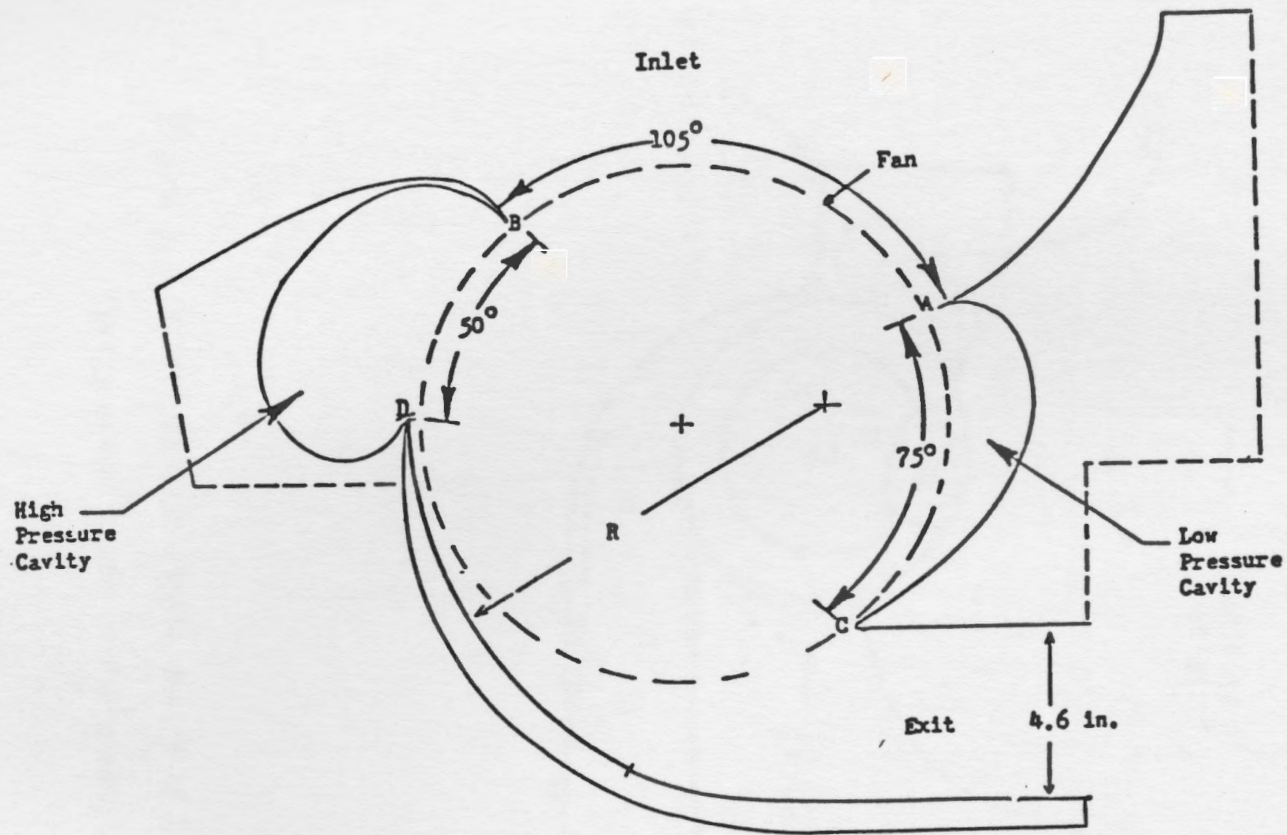


Figure 1.7 Best angular placing of inlet, low pressure cavity, outlet, high pressure cavity. (Ref. 1)

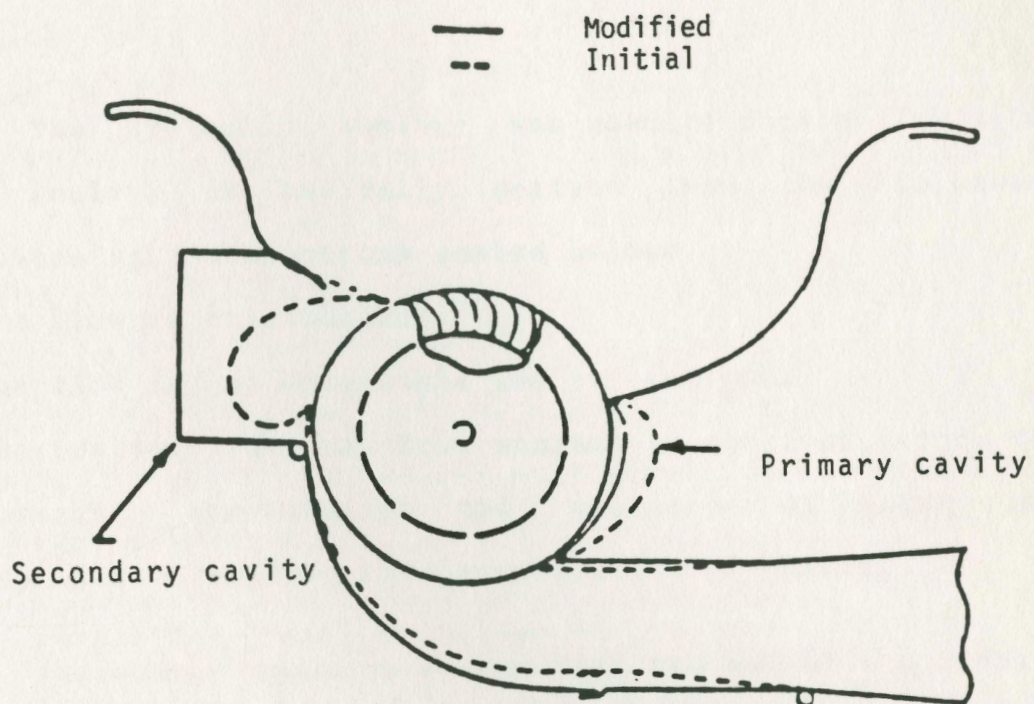


Figure 1.8 Traditional and simple design of C.F.F Secondary Cavity exhibit same performance. (Ref. 4)

CHAPTER 2

HYDRAULIC ANALOGY

The hydraulic analogy was used to obtain flow data. The analogy is basically derived from the following equations with assumptions stated below:

- 1) The flow is frictionless.
- 2) The flow is incompressible and irrotational.
- 3) The pressure on the free surface is constant, and the vertical acceleration and velocity of water are negligible compared with acceleration of gravity.

The energy equation states that the sum of the kinetic and potential energies of a water particle remains constant during its motion. Consider a flow filament originating at point $P(x_0, y_0, z_0)$ (fig.2.1) where the velocity is assumed to be zero (ref.5). The Bernoulli equation applied to any point on the same filament originating at P is given by:

$$p + 1/2 \rho v_w^2 + \rho g z = p_0 + \rho g z_0 \quad 2.1$$

$$v_w^2 = 2 g (z_0 - z) + 2/\rho (p_0 - p) \quad 2.2$$

Since the pressure in a fluid at any point depends

on height of the free surface above that point, therefore:

$$p_o = \rho g (d_o - z_o) \quad 2.3$$

$$p = \rho g (d - z) \quad 2.4$$

By substitution of eq. 2.3 and 2.4 into 2.2 we get:

$$v_w^2 = 2 g (d_o - d) \quad 2.5$$

The water velocity at any point could also be found by measuring the pressure head with a pitot tube and measuring the reference height d_o .

Equation 2.5 may be written as:

$$1 + v_w^2 / 2 g d = d_o / d \quad 2.6$$

The energy equation for 2-D isentropic inviscid gas is given by (ref.6):

$$1 + (\gamma - 1) M^2 / 2 = T_o / T \quad 2.7$$

If the speed of propagation of free surface is given by

$$c = (g d)^{1/2}$$

then equation 2.6 reduces to :

$$1 + v_w^2 / (2 c)^2 = d_o / d \quad 2.8$$

Clearly, if in equation 2.7, the value of $\gamma = 2$ then the two equations for fluid flow and gas flow are analogous. Water tables with a rectangular cross section correspond to $\gamma=2$ and the classical gas flows with p/ρ constant (ref.7). If an analogy is to be obtained between a gas with $\gamma=1.4$ and liquid flow, then a water table with a parabolic cross section should be used, but since the experimental data does correspond well for gases with $\gamma =2$ to liquid flow in a water table of rectangular cross-section, the available water table was not modified.

The analogy relationships are summarized below:

Gas with $\gamma=2$		Hydraulic flow	
Mach Number	= V/a	Froude Number	= V/c
Temperature ratio	= T/T_0	Height ratio	= d/d_0
Density ratio	= ρ/ρ_0	Height ratio	= d/d_0
Pressure ratio	= P/P_0	Square of height ratio	= $(d/d_0)^2$

CHAPTER 3

CONTROL VOLUME ANALYSIS

Consider a control volume in a cross flow fan as shown in fig.3.1.

Inlet area for flow = length of arc ab * dh

Outlet area for flow = length of arc cd * dh

3.1 The Integral Equations

The conservation of mass equation is (ref.8):

$$\frac{d}{dt} \int_{cv} \rho dV + \int_{cs} \rho U \cdot n dA = 0 \quad 3.1$$

and the Conservation of Momentum equation is (ref.8) :

$$\frac{d}{dt} \int_{cv} \rho r C_{\theta} dV + \int_{cs} \rho r C_{\theta} (C \cdot n) dA = \Sigma \tau \quad 3.2$$

Assumptions:

- 1) The flow is steady.
- 2) The flow is incompressible.
- 3) The continuum postulate is valid.

Reduced Equations:

Based on the assumption that the flow is steady, the

first term in both the conservation equation drops out.

The reduced Conservation of mass equation is:

$$r \, d_{\theta 1} \, C_{r1} = r \, d_{\theta} \, C_r \quad 3.3$$

The product of d_{θ} and C_{r1} is the arc length. For a fan with unit span, this product corresponds to elemental area dA .

The reduced Conservation of Momentum Equation is:

$$-\rho \, r \int_a^b C_{s1\theta} \, C_{slr} \, d\theta + \rho \, r \int_c^d C_{d1\theta} \, C_{dlr} \, d\theta = \Sigma \tau \quad 3.4$$

For unit span, the arc lengths at the inlet and the outlet would correspond to areas at the inlet and the outlet.

3.2 The Ideal Velocity Triangle Analysis

Velocity triangles for a C.F.F. at the rotor inlet and outlet are shown in fig. 3.3 with stations indicated in fig. 3.2 for the ideal case where the relative velocity at the suction and the discharge arcs follows the blade contour. The blade velocity at inner and outer radii can be found by using the following equations:

$$U_o = 2 \pi r_1 N \quad 3.5$$

$$U_i = 2 \pi r_2 N \quad 3.6$$

Knowing the blade speed U_0 and the absolute incoming velocity C_{s1} , relative velocity W_{s1} at station s_1 for blade 1 in the suction region can be found by using the following equation:

$$\overline{W}_{s1} = \overline{C}_{s1} - \overline{U}_0 \quad 3.7$$

Relative velocity W_{s2} for blade 1 at station s_2 can be found by using the continuity equation between stations s_1 and s_2 :

$$W_{s1} A_{s1} = W_{s2} A_{s2} \quad 3.8$$

Absolute velocity C_{s2} at station s_2 can then be found by using the following equation:

$$\overline{C}_{s2} = \overline{W}_{s2} + \overline{U}_0 \quad 3.9$$

Assuming that the absolute velocity C_{s2} of the flow discharged at station s_2 remains constant, the absolute velocity of the flow reaching station d_2 in the discharge region will be equal to C_{d2} . Knowing blade angle, absolute velocity C_{d2} and blade speed U_i , the relative velocity W_{d2} can be found at station d_2 using the following equation:

$$\overline{W}_{d2} = \overline{C}_{d2} - \overline{U}_i \quad 3.10$$

Using the continuity equation between stations d_1 and d_2 , the relative velocity W_{d1} can be found at station 1:

$$W_{d1} A_{d1} = W_{d2} A_{d2} \quad 3.11$$

Knowing relative velocity W_{d1} at station d_1 , blade speed U_o and blade angle, the absolute velocity C_{d1} at blade 2 can be found by using the following equation:

$$\overline{C}_{d1} = \overline{W}_{d1} + \overline{U}_o \quad 3.12$$

If incoming absolute velocity increases at the suction arc, the relative velocity would be at an angle of attack to the blade (fig. 3.4). If this angle is very high the blade may stall, preventing a good flow. However, if the R.P.M is increased the relative velocity would become parallel to the blade (fig. 3.4), thus delaying the stall. A decrease in absolute incoming velocity should result in decrease in R.P.M. (fig. 3.5). This suggests that variable R.P.M is necessary for a C.F.F. operation.

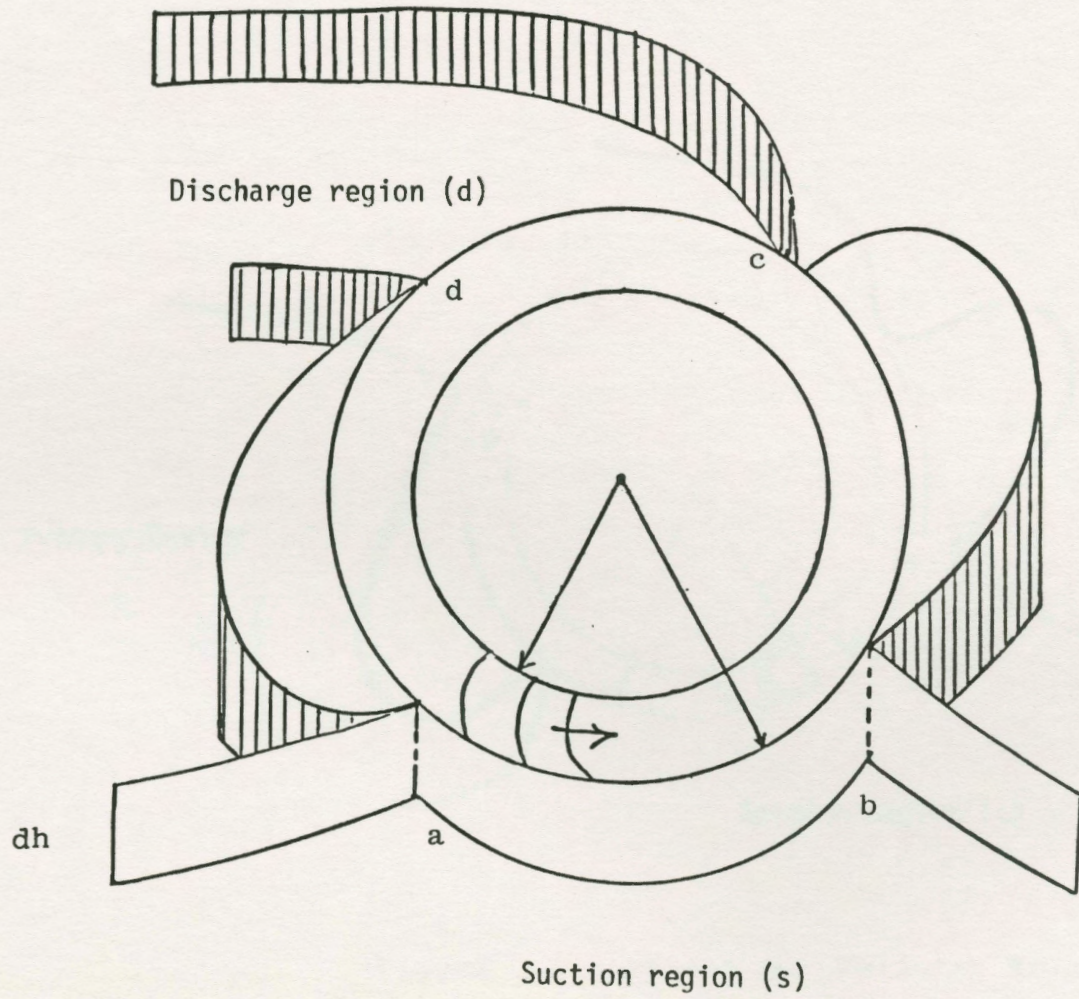


Figure 3.1 Control Volume for A C.F.F.

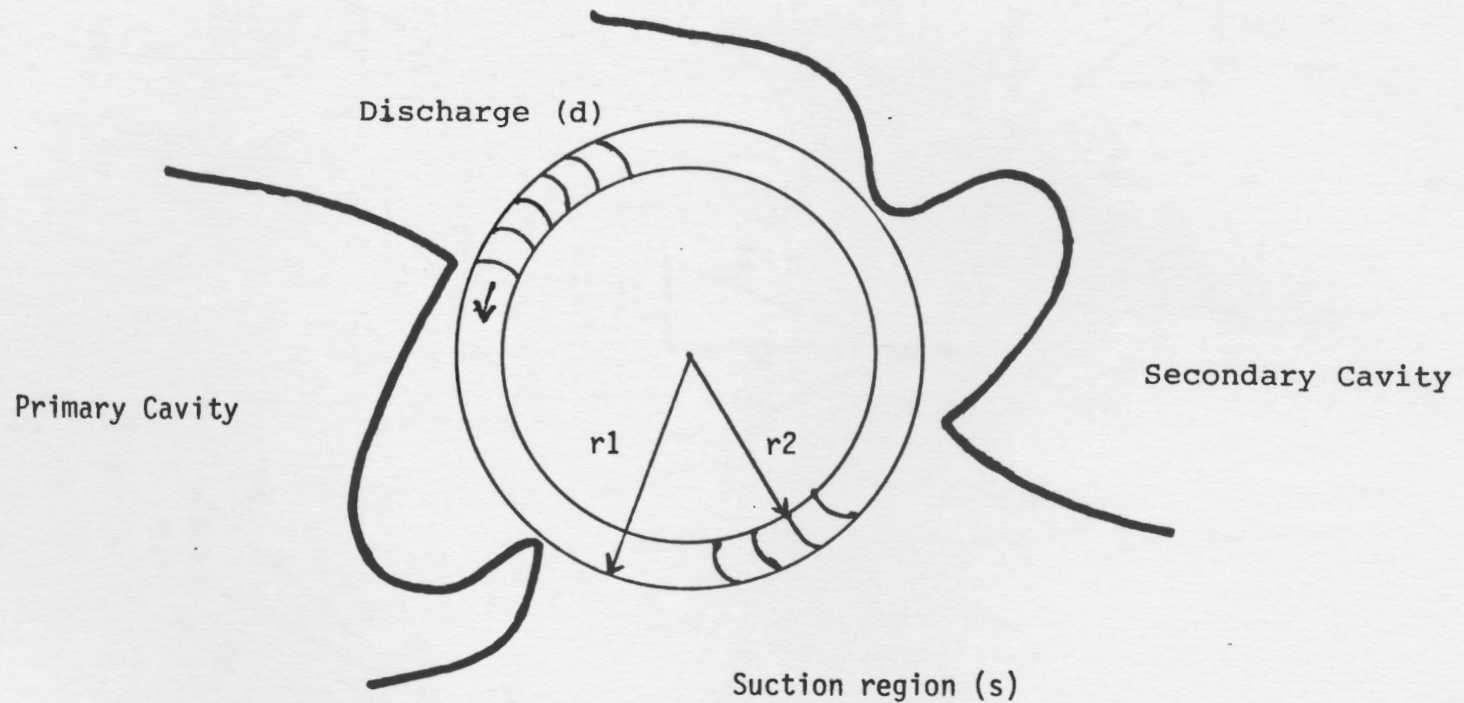
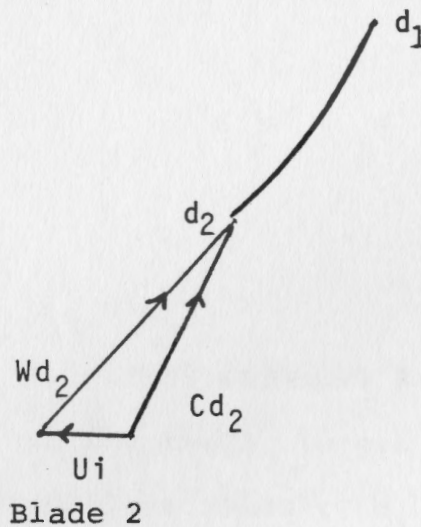
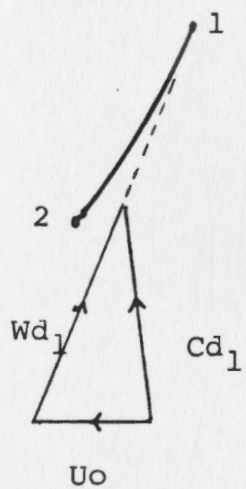
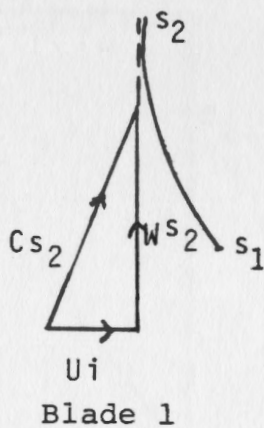
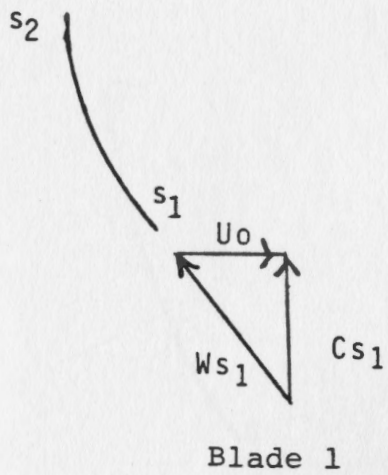


Figure 3.2 Stations for Velocity triangle analysis.



Blade 2

Figure 3.3 Ideal analysis of velocity triangles.

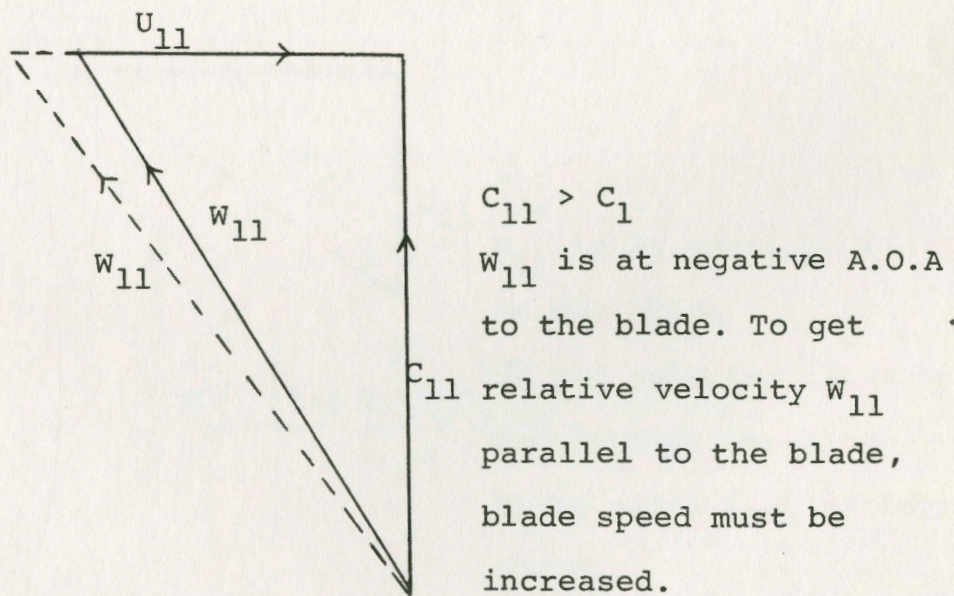
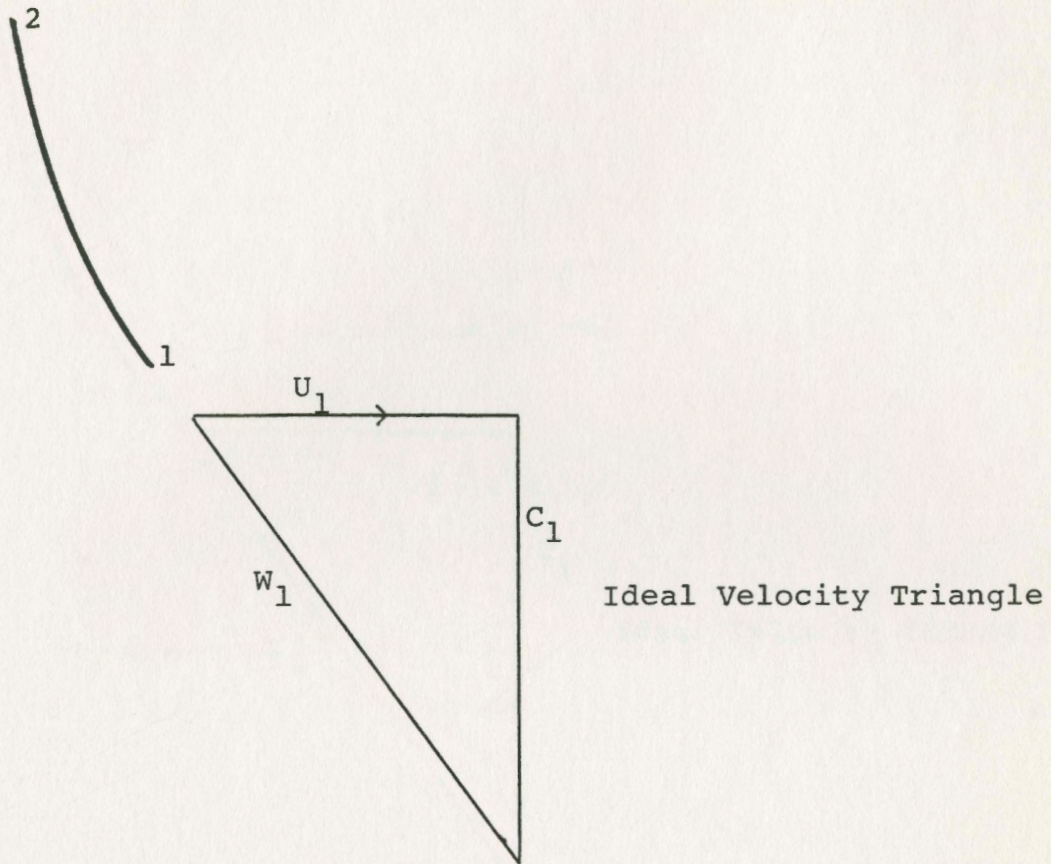
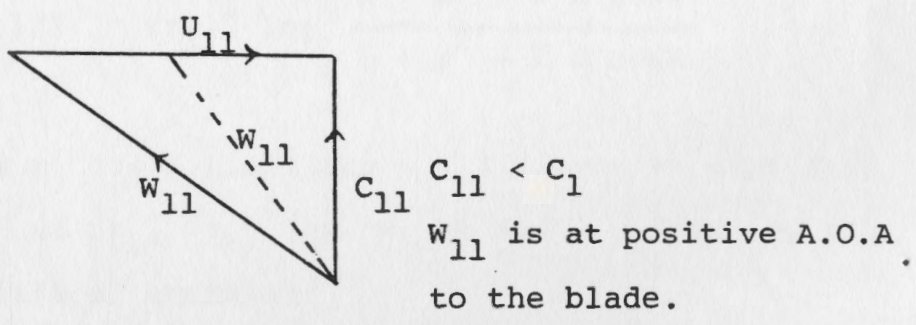
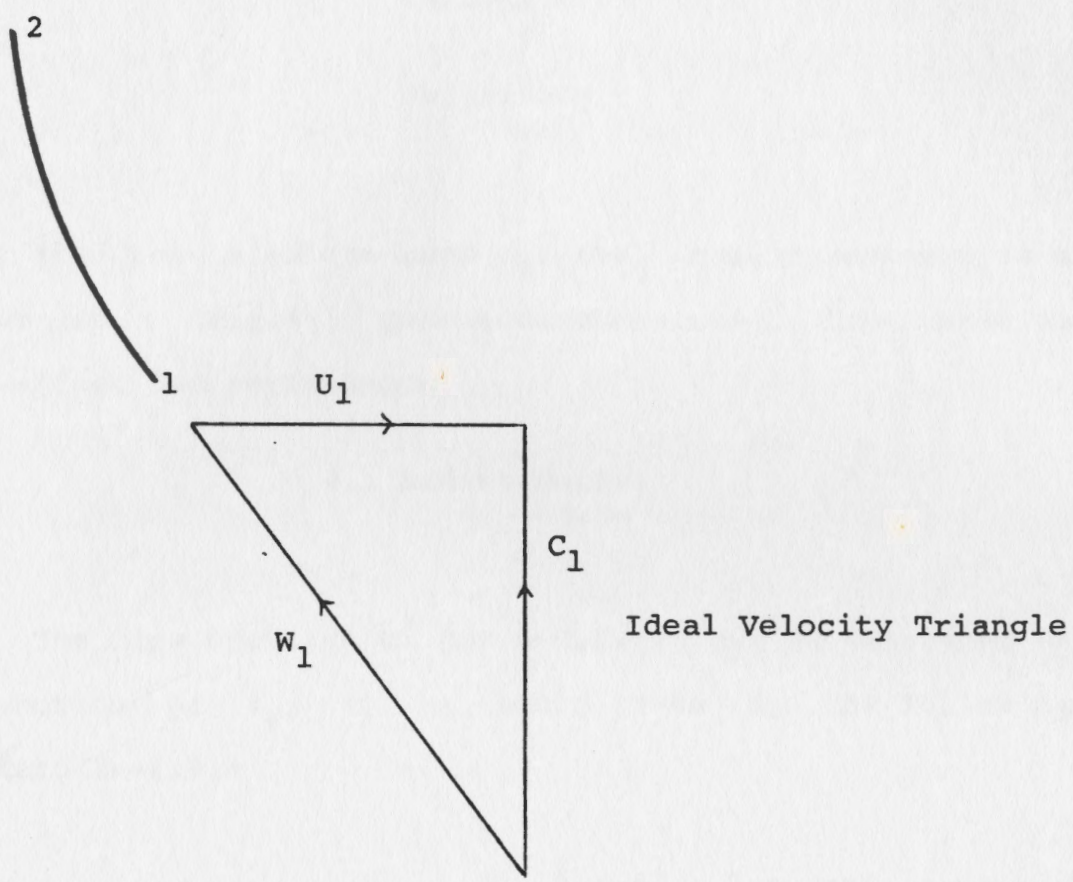


Figure 3.4 Higher incoming absolute velocity requires an increase in blade speed.



To get relative velocity parallel to the blade, blade speed must be decreased.

Figure 3.5 Lower than ideal, incoming velocity requires a decrease in R.P.M.

CHAPTER 4

FAN DESIGN

The Cross Flow Fan used for the present research is a blower fan. Fig.4.1 describes the various fan variables that affect fan performance.

4.1 Radius Ratio:

The flow coefficient for a C.F.F. can be expressed as a function of r_1 , r_2 , a and θ given by the following equation (ref.9):

$$\phi = 1/2 (r_1/r_2)^2 \log \frac{1 + a^2 + 2 a \cos\theta}{1 + a^2 - 2 a \cos\theta} \quad 4.1$$

The pressure coefficient for a C.F.F. can be expressed as a function of r_1 , r_2 , a , θ , β_2 and β_1 given by the following theoretical equation:

$$\psi = 4 a / \left(\log \frac{1 + a^2 + 2 a \cos\theta}{1 + a^2 - 2 a \cos\theta} \right)^{\pi - \theta} \int_0^{\theta} \left\{ (1 + (r_1/r_2)^2)^2 \frac{2 a \sin\theta}{1 + a^2 - 2 a \cos\theta} \cot\beta_2 - 2 \sin n\theta \right\} \frac{\sin\theta}{1 + a^2 - 2 a \cos\theta} d\theta$$

Where $k = - 1/ \log (1 + a)/(1 - a)$

The graphs yielded by the above equations are shown in fig. 4.2-4.4 It is apparent that a high radius ratio implies better performance in terms of ϕ and ψ . Since for aircraft application a C.F.F. should have high value for both coefficients, a high radius ratio is desirable. The present fan has a radius ratio of 0.8. Since J. P. Hancock discarded his original fan radius ratio of 0.9 in favour of a value of 0.7 to improve design performance; a reduction in radius ratio would lead to:

- 1) Reduction in internal losses because of an increase in blade passage Reynolds number,
- 2) Improvement in the structural integrity of the fan.

Therefore, the radius ratio of 0.8 is used as the starting design.

4.2 Solidity

Solidity of a fan is defined by the ratio of fan chord to blade spacing. Solidity of the fan involved in this research is 1. Solidity should not be very high because it could result in lesser through flow due to the space occupied by the blades. Also, it could result in more weight if a large number of blades are used in the fan. A

lower value of solidity would result in a loss of channel action. Also if a high solidity value is obtained by increasing chord length, the area reduction at inlet and area increment at outlet would accenuate (fig. 4.5). This implies that the flow will pass through a nozzle at the inlet and through a diffuser at the outlet. Clearly such an arrangement is not sought for Airplane application as it implies an increase in static pressure over the upper surface and hence a decrease in lift. The solidity value of 1 for the present fan is considered acceptable as the starting design.

4.3 Blade Discharge Angle

Based on the velocity triangle analysis described in section 4.2, the blade discharge angle should affect the fan performance considerably. A variable R.P.M fan should be used so that relative velocity (obtained by subtracting blade speed from absolute incoming velocity) would always be at a small angle of attack to avoid flow separation. According to Harloff's analysis, fans with values of β_0 greater than 70° generally perform better. Discharge angle for the present fan is 45° .

Very few researchers have stressed the blade discharge angle. Harloff and Hancock's analysis with graphs shown in

fig. 4.2-4.4 are used for justification of present value of discharge angle. Only one of Harloff's fans had β_0 of 45 and this fan did not perform well. This very fan had a very low solidity compared to his other fans, therefore bad performance cannot be attributed just to the high value of β_0 . However, Hancock's analysis and the graph shown in fig.4.2-4.4 suggest that a low value of β_0 is good for high pressure coefficients. Therefore, a low discharge angle is desirable. Present value of β_0 therefore seems an acceptable compromise.

4.4 Cavity Design

The cavities may be designed as part of the fan housing to capture the primary and secondary vortices. In the arrangement shown in fig.4.6, the primary vortex must be counter-clockwise and the secondary vortex must be clockwise to help the radially incoming flow change to radially outgoing flow. The primary vortex, in effect, acts as a seal against the return flow that the fan might pick up. The secondary vortex helps in reducing transition losses. The primary vortex is a low pressure vortex whereas the secondary vortex is a high pressure vortex.

Dalin and Ilberg and Sadeh (ref.3) have suggested that the primary vortex influences the fan performance more than

the secondary vortex, therefore the wall or cavity containing this vortex should be carefully designed. Porter and Markland (ref.2) have suggested that the outer wall has the greatest influence on the vortex positioning. According to Harloff (ref.1) both cavities affect the performance, but the low pressure cavity is more sensitive. Since the flow and pressure coefficients can be maximized by pushing the vortex center as close to the impeller outer periphery as possible (ref.3), the cavity design can be done empirically or by following established shapes as closely as possible to achieve the optimum cavity shapes.

4.5 Dimensional Analysis

Because of the two dimensional nature of the Cross Flow Fan, its dimensional analysis is slightly different from conventional pumps or fans. In a C.F.F., the pressure head is a function of discharge rate, R.P.M, density, viscosity, roughness and hydraulic diameter instead of the geometric diameter. Since the inlet in a C.F.F. is 2-D, the pressure head is a function of span also. The hydraulic diameter encompasses both span and diameter as defined by :

$$D_h = 2 S D / (S + D)$$

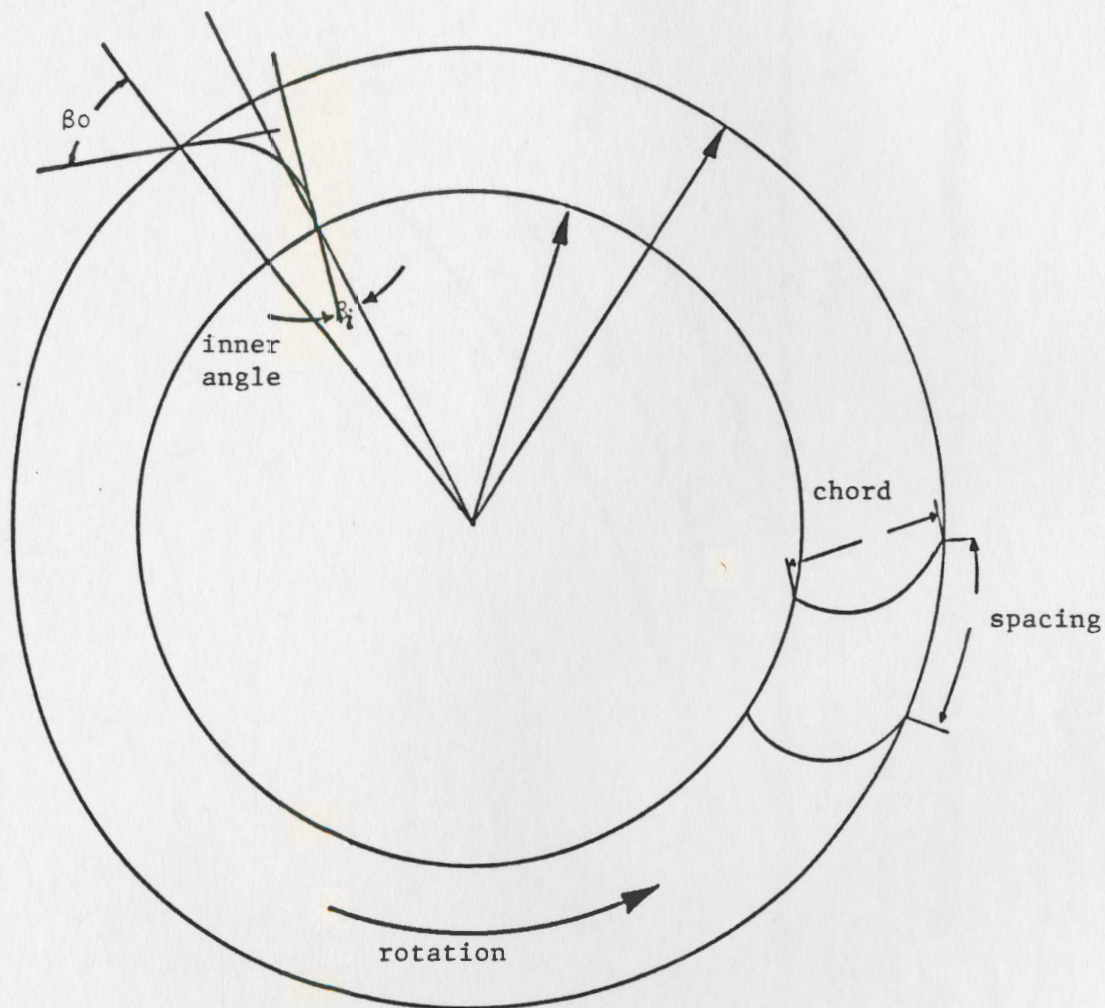
4.1

If we assume a functional relationship between the physical variables of the fan, then:

$$f_1 (gH, \text{bHP}, Q, D_h, N, \rho, \mu, \epsilon, V) = 0 \quad 4.2$$

A dimensional analysis of the problem yields the following pertinent parameters:

Capacity Coefficient	$C_q = Q/N D_h^3$
Power Coefficient	$C_p = \text{bHP}/(\rho N^3 D_h^5)$
Head Coefficient	$C_h = gH/(N^2 D_h^2)$
Roughness Ratio	$RR = \epsilon/D_h$
Reynold's Number	$Re = \rho N D_h^2/\mu$
Non Dimensional Velocity	$NDV = V/N D_h$



Variables:

$$\beta_o = 45$$

$$\beta_i = 10$$

$$r_i/r_o = 0.8$$

$$\text{Solidity} = 1$$

Figure 4.1 Fan Variables

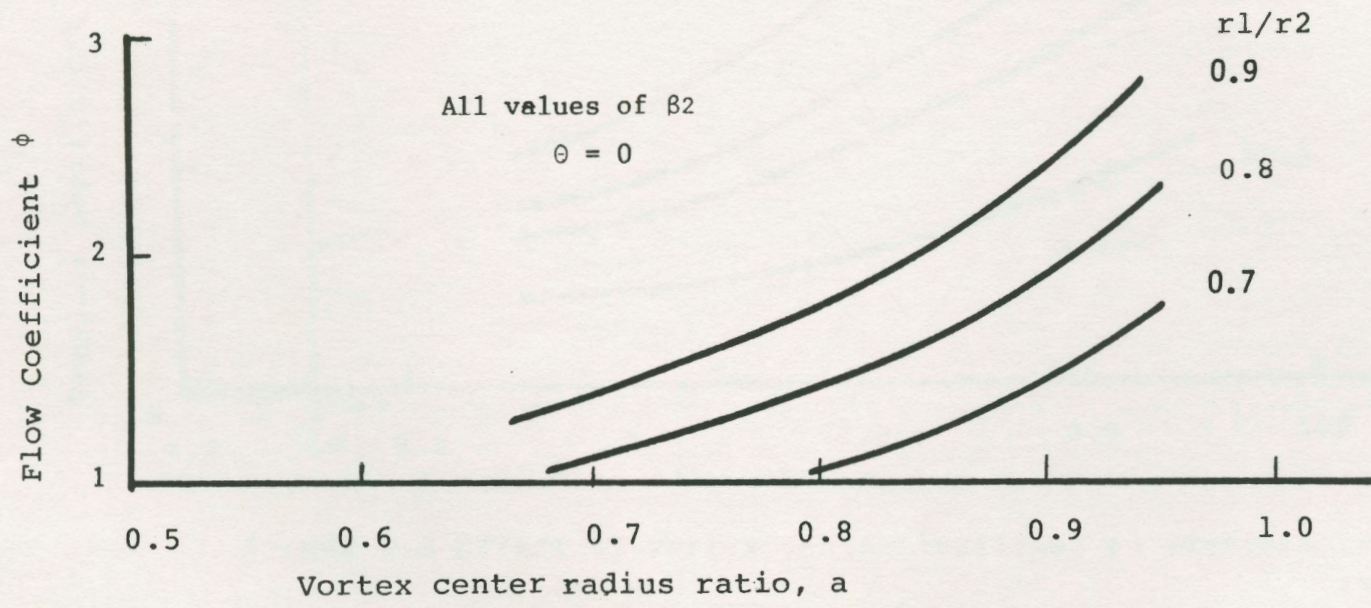


Figure 4.2 Effect of vortex center location on flow coefficient.

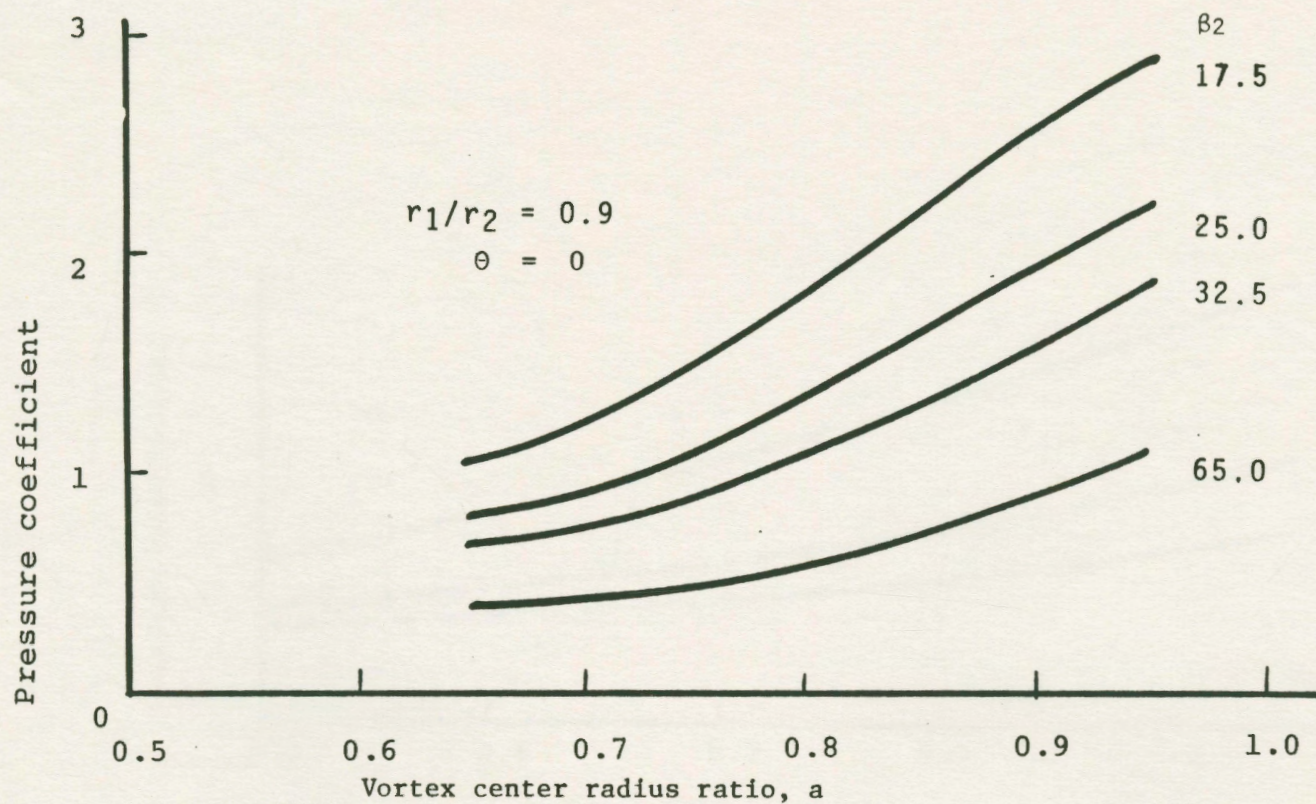


Figure 4.3 Effect of vortex center location on pressure coefficient.
(Ref. 4)

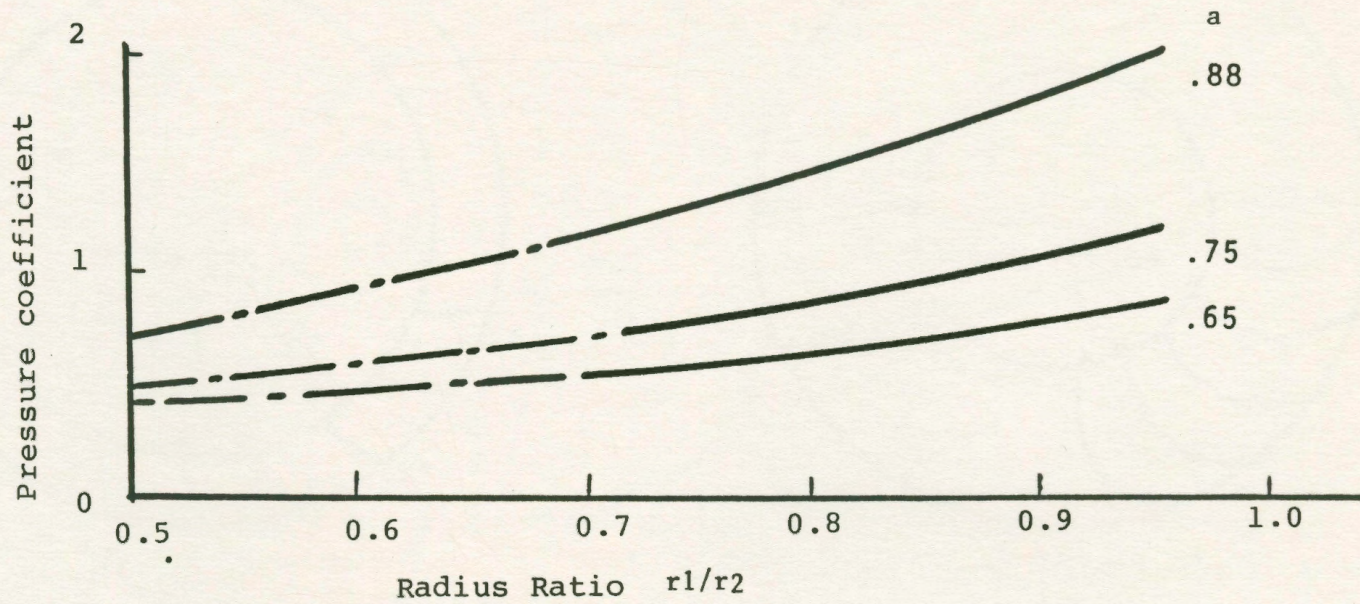
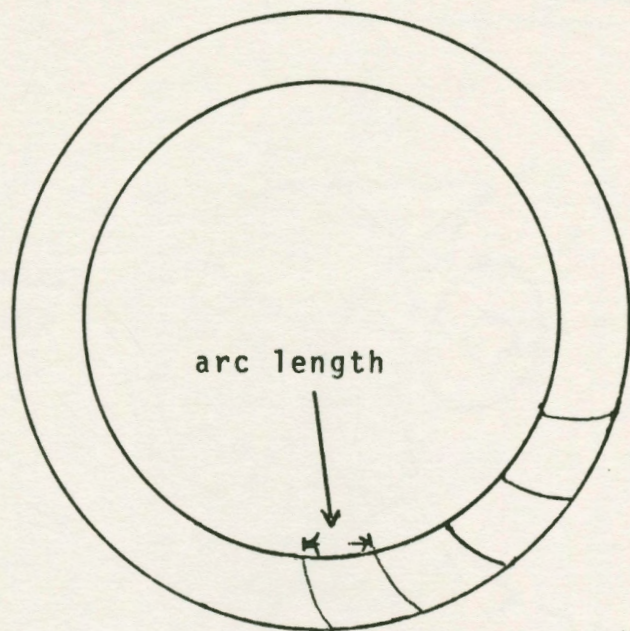
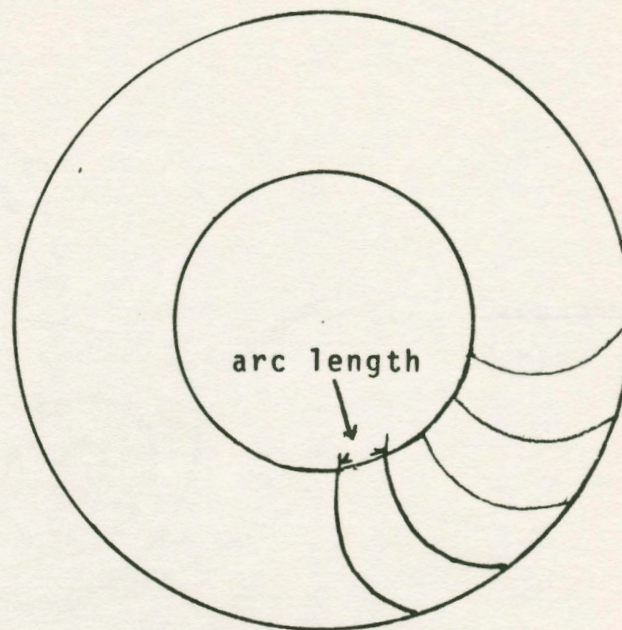


Figure 4.4 Effect of Impeller radius ratio on Pressure Coefficient (Ref. 4)



Fan 1



Fan 2

For same span fan 1 has greater inner area than fan 2, because inner arc length between two consecutive blades reduces for a smaller inner radius.

Figure 4.5 Longer chord resulting in accentuation of nozzle action.

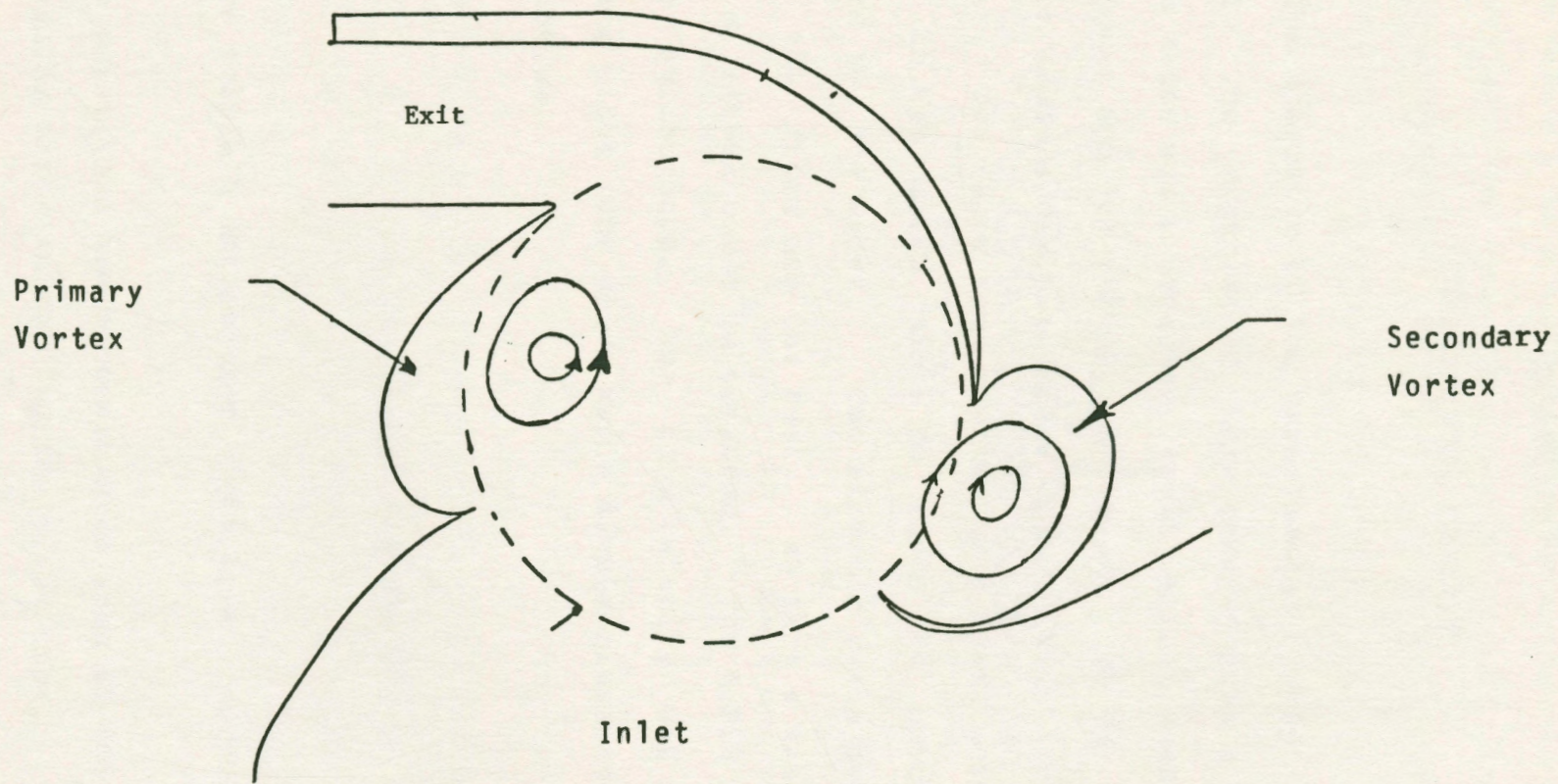


Figure 4.6 Direction of vortices for a good through flow.

CHAPTER 5

EXPERIMENTAL PROGRAM

The schematic of the experimental setup is shown in fig.5.1. The experiments were conducted on a water table. The fan motor was a variable speed motor rated at one half horse power and 500-5000 R.P.M in air. At the water level at which experiments were performed, it gave about 370 R.P.M in water. The motor was mounted on a frame work which was placed on the water table so that the motor shaft was extended in the water. The airfoils were made into two parts, the front and the rear, so that a large range of angles of attack could be obtained. The R.P.M was measured using a stroboscope. The flow velocity was measured by using the pitot tube which was a simple glass tube bent into an L section.

5.1 Sources of Error

The possible errors that might have occurred are listed below.

- 1) The pitot tube had a constricted area at the bend.
- 2) Parallax error in reading the pitot tube.
- 3) At high angles of attack the flow from leading edge of

the airfoil to its trailing edge seemed to pass through a diffuser on the upper surface and a nozzle on the lower surface as shown in fig. 5.2. Any velocity decrement on upper surface could be partially due to this fact.

5.2 First Design

A NACA 0018 section airfoil was made out of balsa wood and the cross flow fan was installed at the maximum thickness position (fig.5.3). Any blowing arrangement installed in wings should be placed as close as possible to the leading edge (ref.11) to obtain a value of momentum coefficient that will result in highest increase in lift.

The momentum coefficient is defined as:

$$C_{\mu} = \frac{\dot{m} V_j}{q_{\infty} S}$$

The reason that the fan is not installed even further forward on the airfoil is purely dimensional. Installation of this fan further towards the leading edge would have meant a further enlargement of the already oversized airfoil.

5.3 Housing

The two housings used in the first design were made out of plastic because of the easy shapeability of this material. However when tested in water table they vibrated substantially with the fan on.

Since the primary purpose of a housing is to obtain the desired flow, this design was discarded at the start as the housing followed the shape of flow instead of forcing the flow in the desired direction. The new housing was made of fiber glass and foam. Since the airfoil was divided into two parts, the housing along with the airfoil could be tested at a number of different angles. Except for one particular angle, the flow was bad. It spilled on both the upper and lower surfaces and resulted in premature separation. The fan was observed to carry a big elliptical shaped cavity along with a central vortex (fig.5.4). No flow passed through this cavity. No vortices were trapped and no through flow was obtained.

With the airfoil at one nose low position, the fan picked up the flow from lower surface and discharged it on the upper surface. At the same time, the inlet picked up flow from the rear direction on lower surface (fig.5.5); this flow should be considered advantageous for the improvement of lift (ref.12). According to authors of ref.

12 any circulation in the physical sense increases the momentum coefficient. Lift augmentation at lower values of momentum coefficient is due predominantly to boundary layer control. Higher lift augmentation is achieved through enhanced circulation. Without a sharp trailing edge, the Kutta condition no longer fixes the circulation strength. The circulation and leading and trailing edge stagnation points are controlled by jet momentum. The graph shown in fig. 5.6 suggests that high values of momentum coefficient lead to high values of lift coefficient at the same angles of attack.

The spillage on upper and lower surface was observed to change direction with a change in the angular position of the airfoil. This can be made use of for thrust vectoring.

Since the inlet and outlet designs were not very good and cavities did not effectively trap the vortices, a new model was made.

5.4 First Modification

To catch the vortices efficiently, one of Harloff's best angle placings of inlet arc, high pressure cavity, outlet and low pressure cavity as shown in fig.5.7 was followed. The inlet and exit had better contours as shown in fig.5.8.

The tests were run on the water table with the same fan and water speed. The secondary vortex was trapped immediately in the high pressure cavity and could be seen clearly (fig.5.9). The primary vortex could not be trapped and therefore, the flow was uncontrolled. There was spillage on both upper and lower surfaces, which indicated the absence or wrong positioning of the primary vortex resulting in return flow. The fan picked up flow even from the exit when the primary vortex was absent or not positioned correctly. Suction was observed from upper surface leading edge (fig.5.9). No suction was observed from the lower surface. Even if the inlet was shut altogether with a plastic sheet (fig.5.10), the flow pattern of the system remained absolutely the same. The fan in essence picked up the flow from the upper surface leading edge, circulated it and exhausted it over the trailing part of upper surface. Various angles of attack were tried (fig.5.11,5.12). The flow did improve at higher angles of attack i.e there was suction from lower surface, but there was still too much spillage on the lower surface. The primary reason for all this seemed to be the absence of the primary vortex. In an attempt to capture the primary vortex, a second modification was made to the second airfoil.

5.5 Second Modification

The primary cavity needed to be redesigned. Since J.P. Hancock's fan housing seemed to have a shallower rear cavity, the primary cavity was filled up to make it more shallow (fig.5.13). A shallower cavity in essence would not contain the whole vortex, in effect it would result in reduced through flow. Since the primary aim at this time was to be able to see this vortex, a new design with a shallower cavity was employed. No vortex formation in the primary cavity was observed. Its absence was obvious from spillage at the inlet as the fan picked up the return flow. No suction was observed at the inlet. The flow essentially remained the same as that of the last design. The primary cavity was then redesigned.

5.6 Third Modification

The primary cavity was made deeper than the first design (fig.5.14). The primary vortex was caught immediately but it rotated in the wrong direction (fig.5.15). There was no suction from the lower surface (fig.5.15). The flow was still being spilt on the upper and lower surfaces. Even with the inlet closed, the flow remained the same (fig.5.16). The flow was observed closely and it was found

that the trailing edge of the primary cavity received the fan flow first and then the flow followed the cavity shape in the wrong direction. By shutting down a small part of the trailing edge to the incoming flow with a plastic sheet the flow changed its direction (fig.5.17). The primary vortex was then correctly caught (fig.5.18). In this design, both vortices were trapped, they were correct in their direction of rotation, but still no flow was picked up by the fan at the inlet (fig.5.18). The flow speed seemed too high, so a modification was made by changing the fan motor.

5.7 Low R.P.M Experiment

Since in the previous experiments the fan spilled too much flow, it was realized that probably the fan speed was too high. A new 1/36 HP motor was used in place of the earlier 1/2 HP motor. It gave about 90 R.P.M in water. This motor was installed in the setup of final modification. Some spillage was observed at the inlet (fig.5.19) but stopped at low angles of attacks instantaneously (fig.5.20). The fan picked up flow from the leading edge as could be seen by the powder flow from the inlet to the outlet. Suction was observed from upper surface leading edge (fig.5.19). Above all this configuration seemed to work

excellently for boundary layer control. Streamlines were observed to move towards the airfoil when the fan was switched on. At angles of attack where the flow was separated on the upper surface (fig.5.21), the flow streamlines were observed to move towards the airfoil when the fan was switched on (fig.5.20). The secondary vortex was very weak. The primary vortex was observed to have its center outside the periphery of the fan (fig.5.19).

5.8 Inlet Modification and Chord Reduction

The chord of the rear part of the airfoil was reduced so that the jet thickness and physical thickness added up to the original thickness of the airfoil (fig.5.22). This implies a reduction in weight and hence the weight addition because of the fan installation can be compensated. Also the air blown over the upper surface is more streamlined.

The new inlet was designed (fig.5.23) to take into account the fact that maximum throughput can be obtained if flow coming in is radial in direction. Much better suction compared to previous designs was observed, because of the new inlet design, the flow could be picked up from behind the inlet also. This can be substantiated by theoretical analysis of flow through a C.F.F., which has a streamline pattern as shown in fig.5.24. Both the vortices were very

weak, possibly because of the low fan R.P.M. Velocity data were taken for this modified airfoil at various angles of attack (fig. 5.25-5.29). The pressure coefficient C was plotted on the upper surface along chord stations (fig. 5.31-5.33). A clear increment in magnitude of pressure coefficient was observed at all angles of attack.

Momentum coefficient was calculated and it was observed to change in magnitude with change in angle of attack (fig.5.33). Higher values for momentum coefficient were obtained with the fan running. Recall (fig.5.6) an increase in momentum coefficient leads to an increase in lift coefficient.

At this stage however, one thing was evident the fan seemed to be too big for the airfoil. To get any flow improvement the next step would be to reduce the fan size.

5.9 Smaller Fan Experiment

A blower fan of dimensions given in fig.5.34 was used for the next modification. Both vortices were captured correctly in this arrangement (fig.5.35). The primary vortex was observed to have its center inside the fan periphery. Without a casing, the vortex center seemed to lie very close to shaft center and it was observed to move circumferentially, but when the rear part of the airfoil was

brought closer, it was observed to stabilize at the position shown in fig.5.35. It seemed the secondary cavity was not really necessary. As it seemed with only the rear part present, the fan did not pick up flow from that direction (fig.5.37). The argument in favour of the secondary cavity is that it captures a vortex which is clockwise in direction and hence can enhance the through flow in the fan. The inlet and exit seemed better suited to this fan's smaller size.

The fan flow was observed at various angles of attack. The fan performed well for a large range of angles of attack (fig.5.38, 5.39). Velocity data was taken at various angles of attack and a clear increase in velocity was observed with the fan running (fig.5.40-5.43). Momentum coefficient was calculated at the above angles of attack (fig. 5.33). It attained values as high as 1.

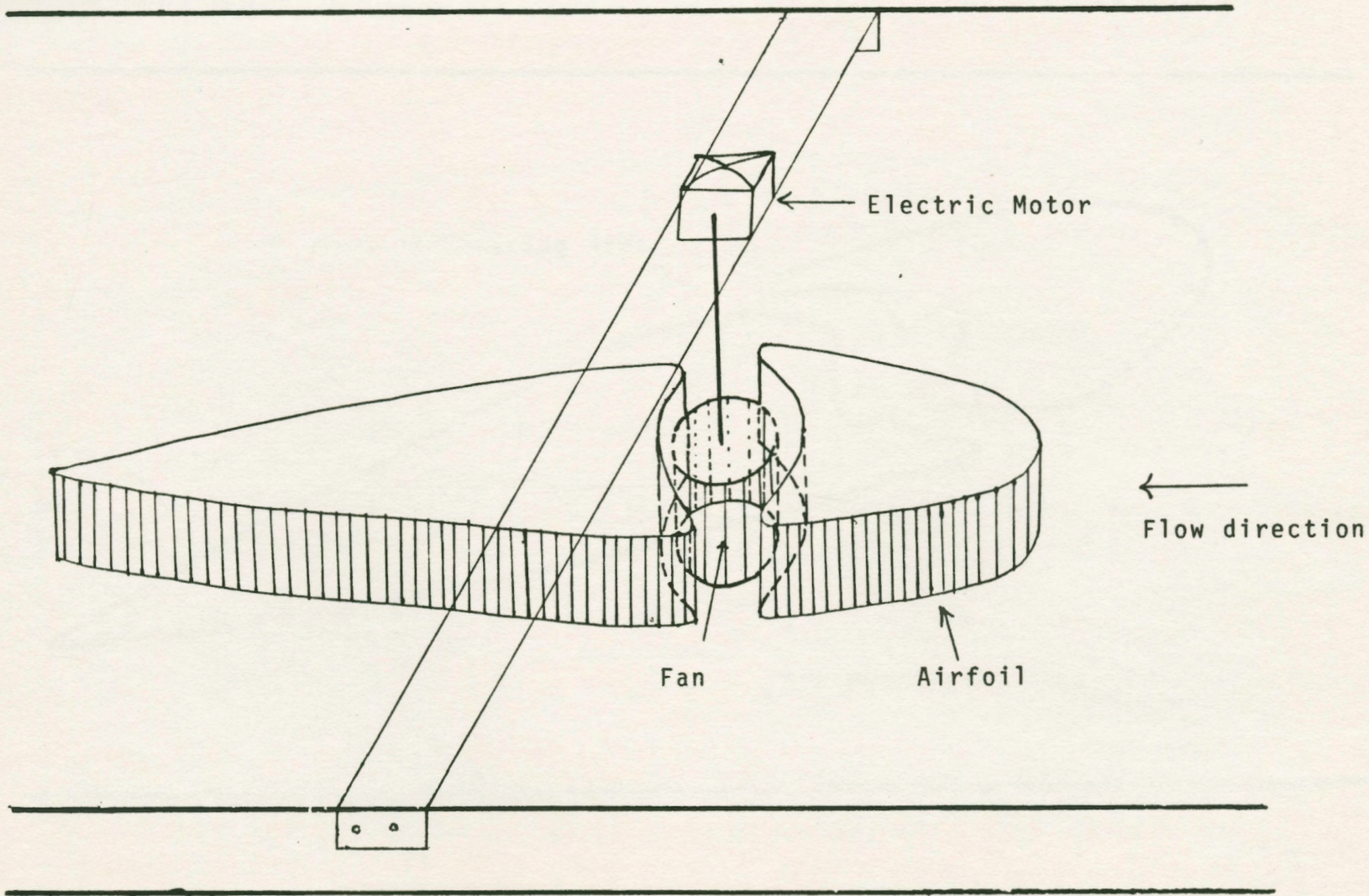


Figure 5.1 Experimental setup in the water table.

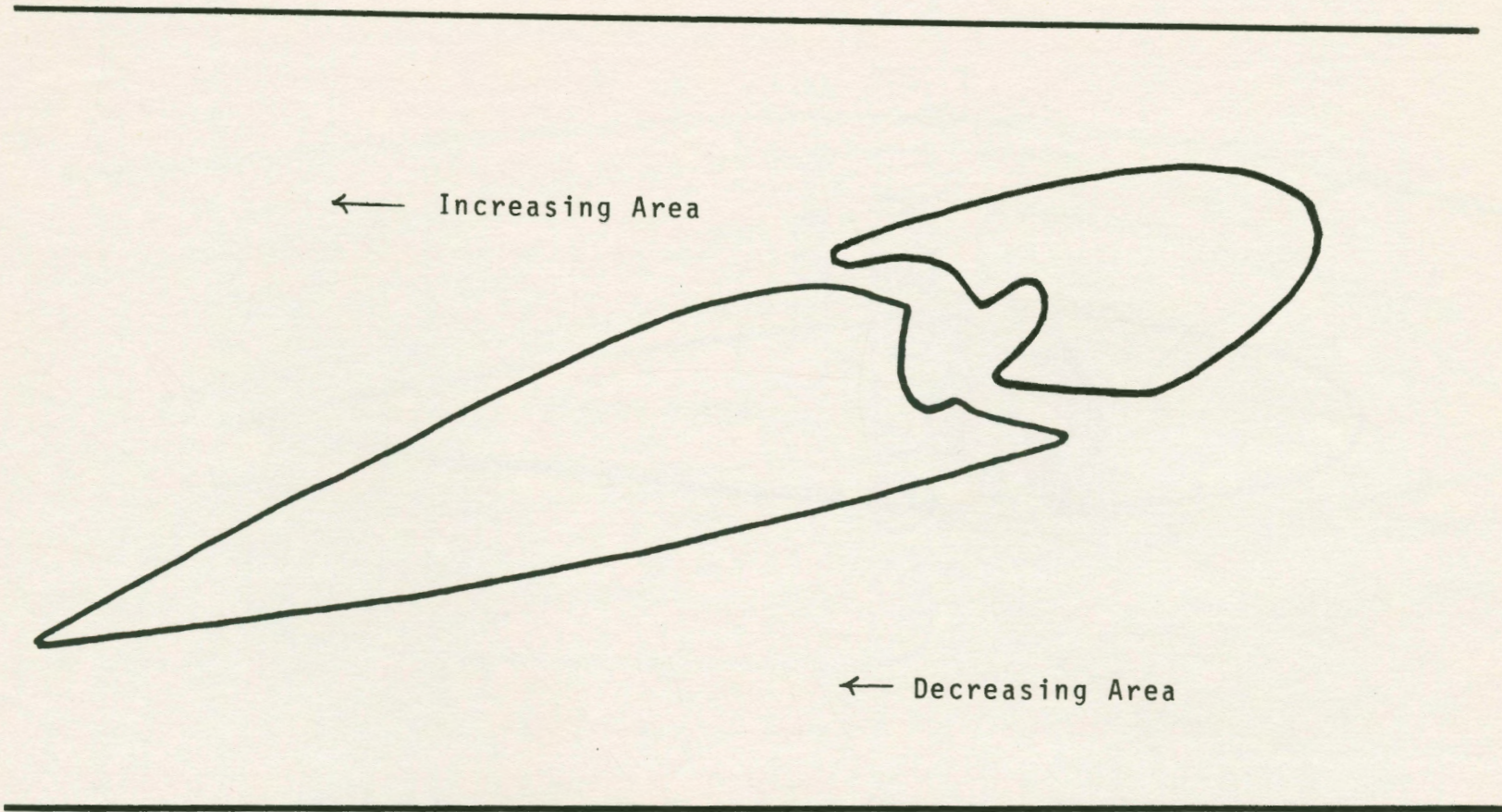


Figure 5.2 Airfoil dividing water table into diffuser and nozzle.

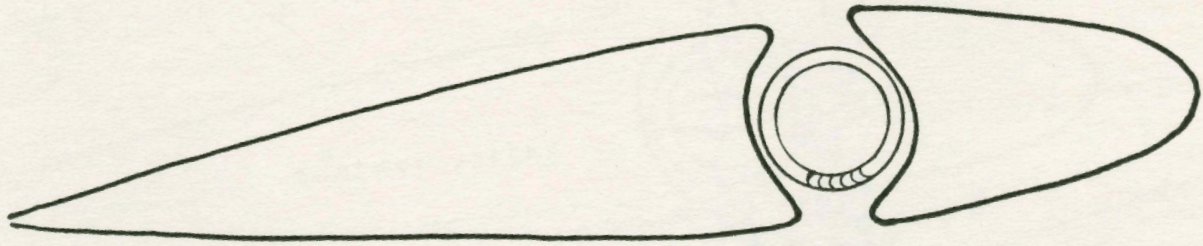


Figure 5.3 First Design, Fan Installation at maximum thickness.

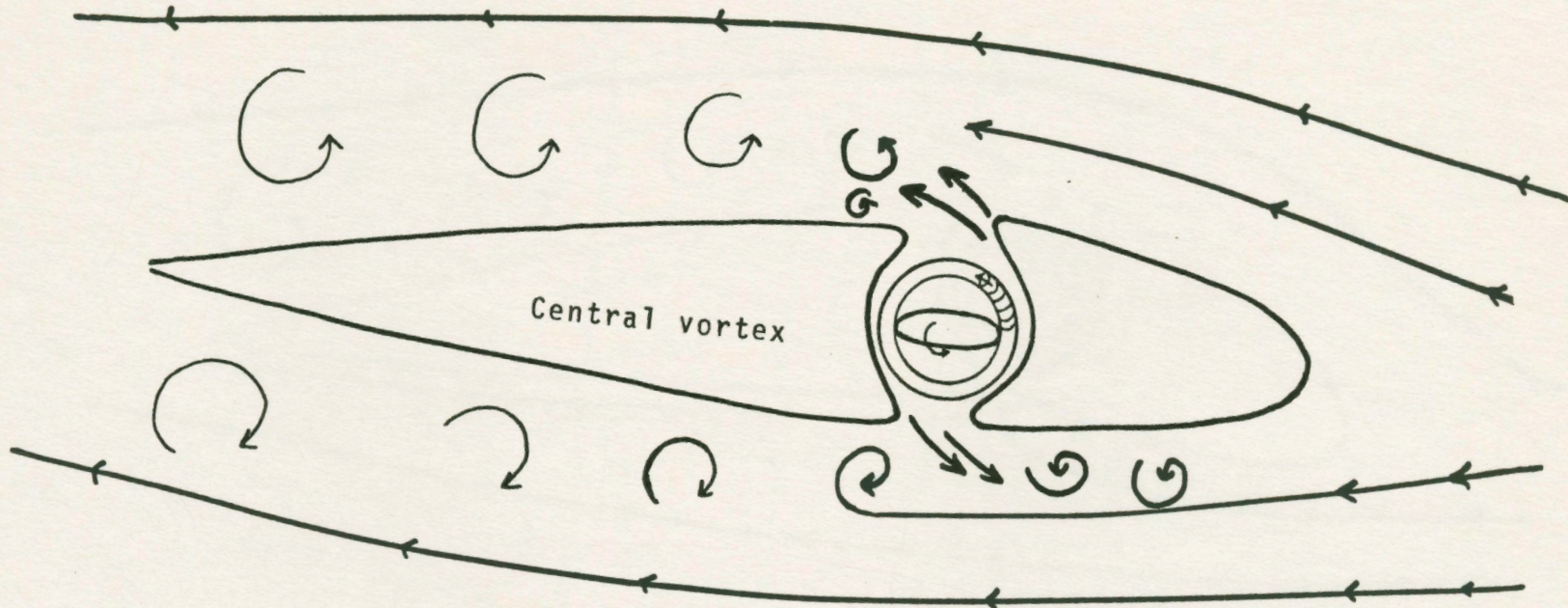
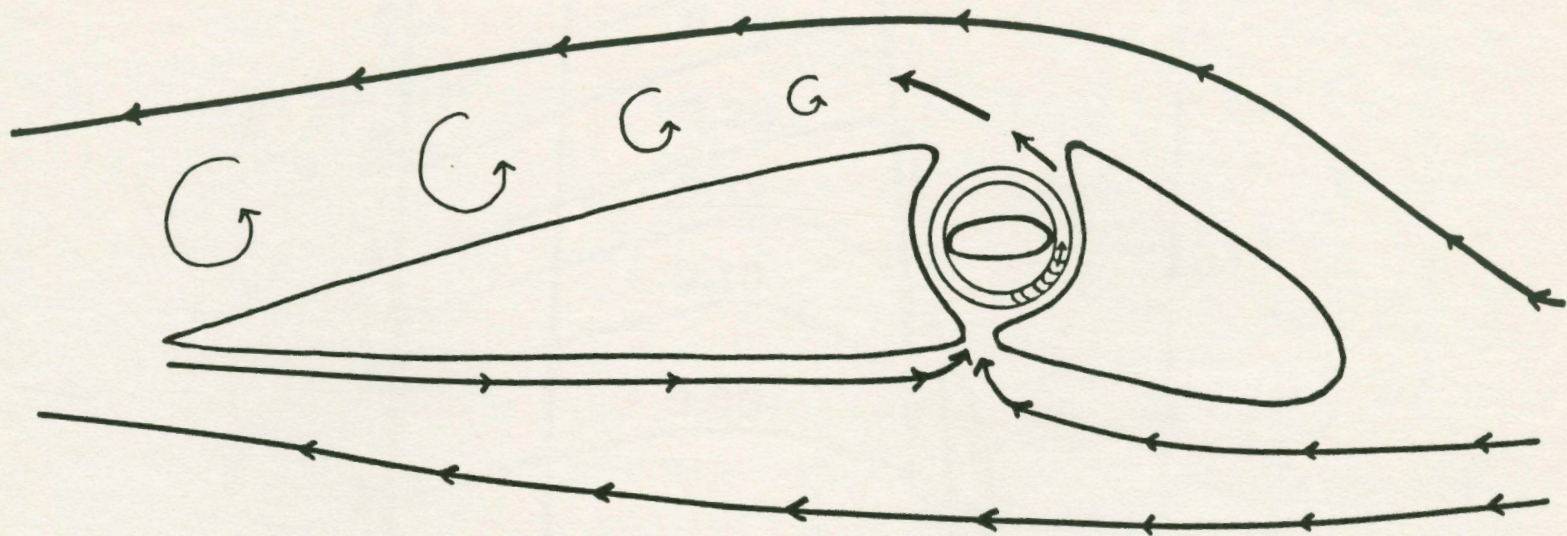


Figure 5.4 First Design with elliptical cavity and return flow at inlet.



- . No return flow
- . Spillage at outlet

Figure 5.5 First design at nose dip placing.

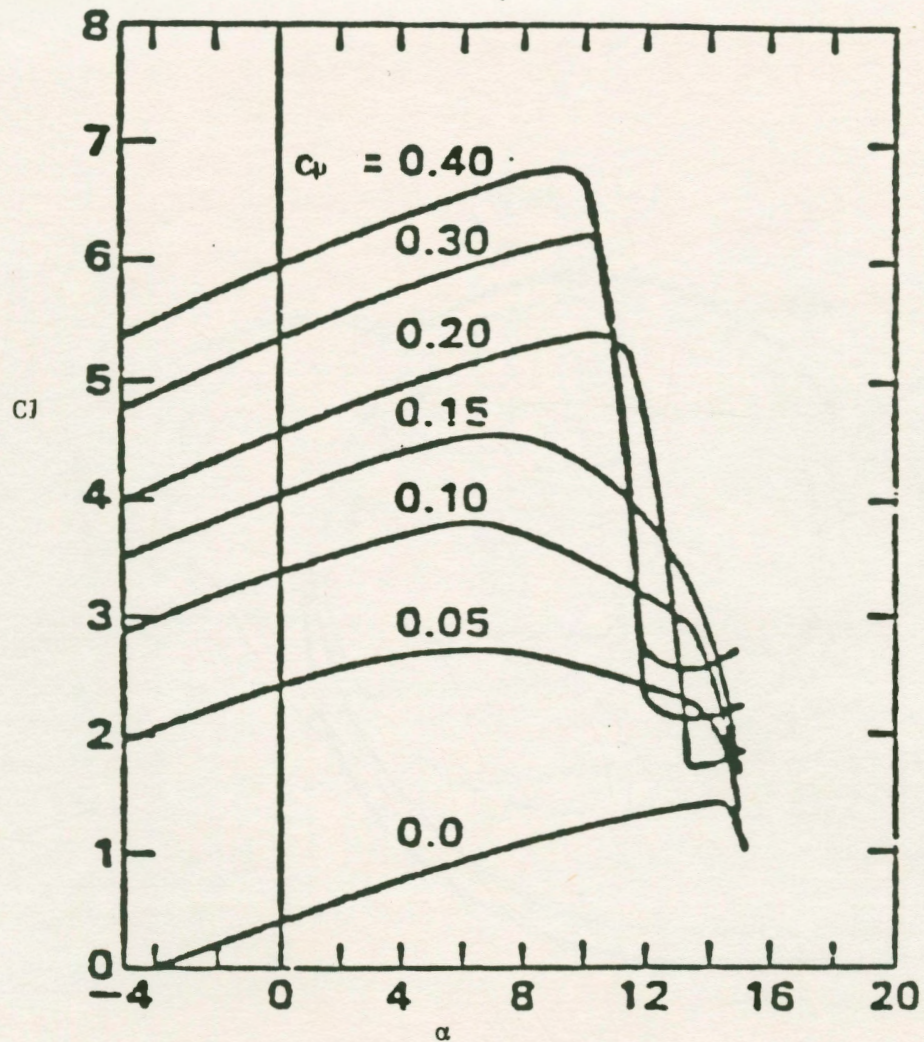


Figure 5.6 Higher momentum coefficient leading to higher lift coefficient at same angles of attack.

(Ref. 12)

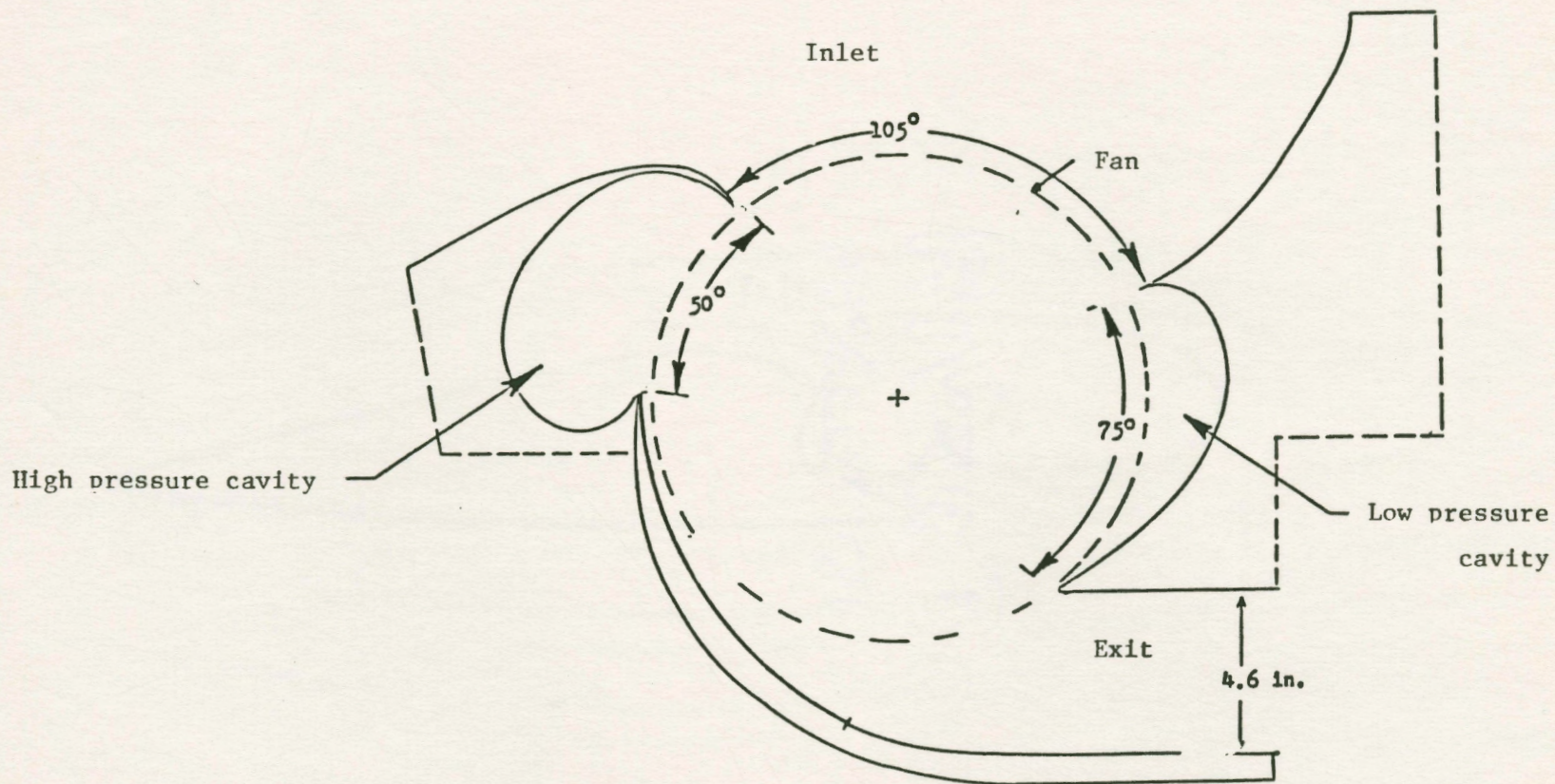


Figure 5.7 Best angular placing of the inlet, low pressure cavity, exit and high pressure cavity.

(Ref. 1)

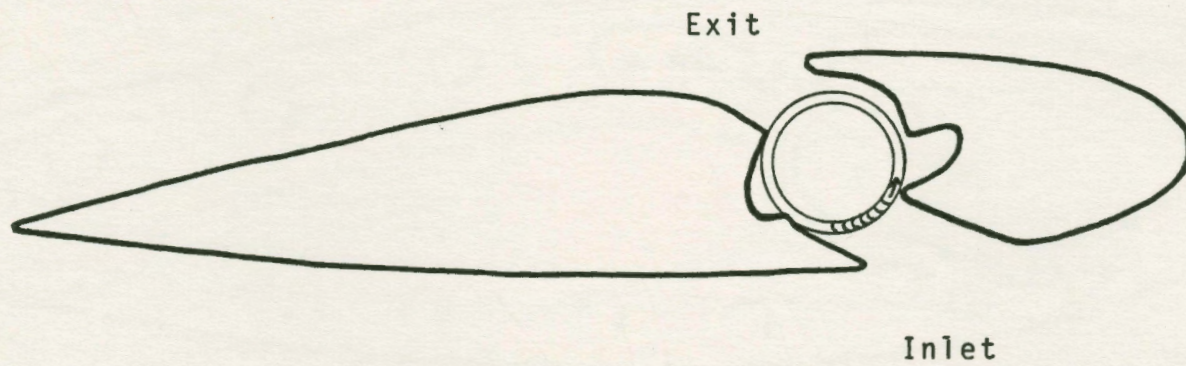


Figure 5.8 New Inlet and exit design.

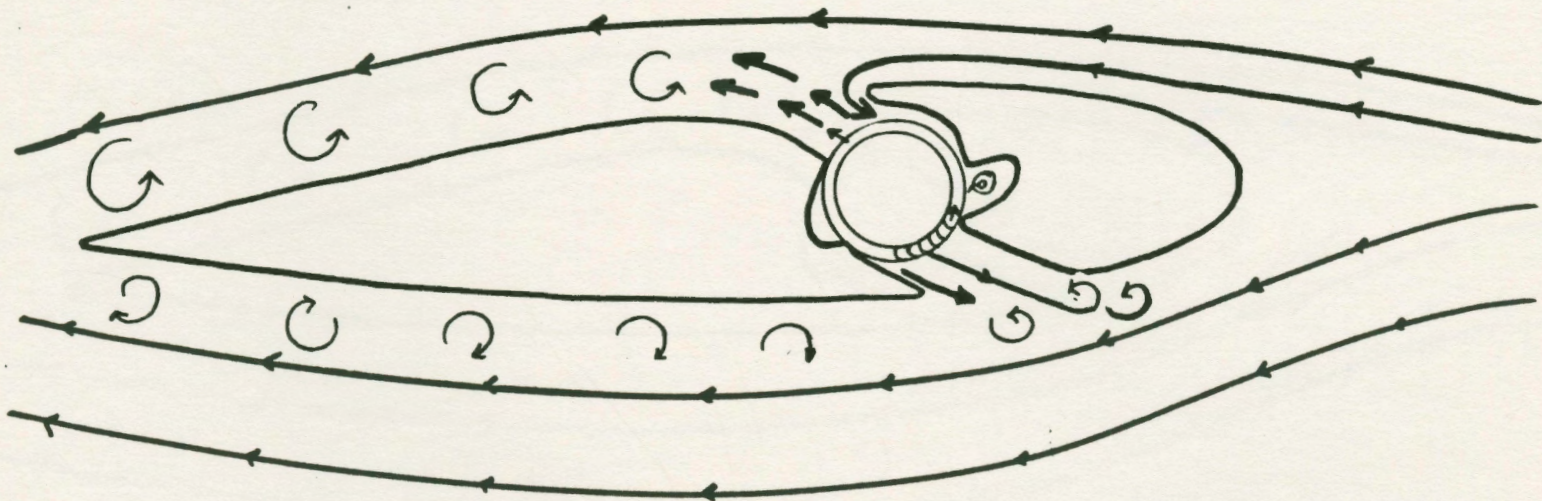
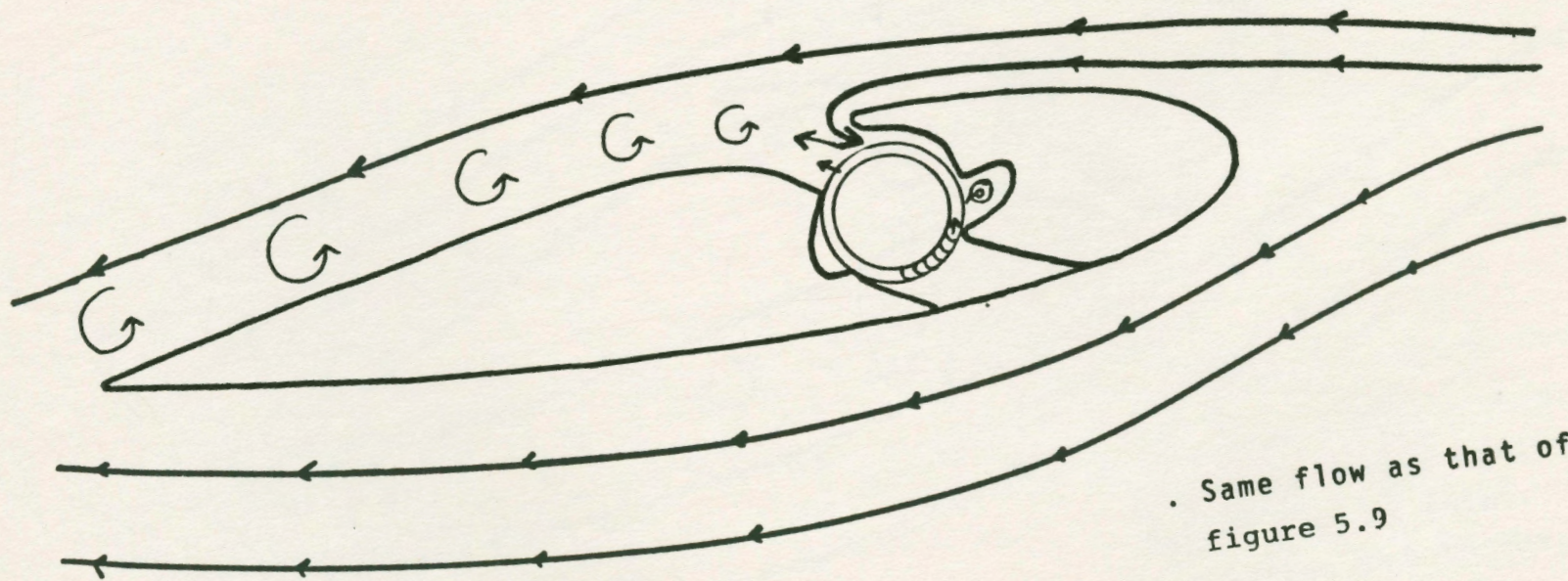


Figure 5.9 First Modification at $\alpha = 0^\circ$

- . Secondary vortex trapped.
- . Suction from leading edge U/S.
- . No suction from L/S.
- . Return flow at L/S.



. Same flow as that of
figure 5.9

Figure 5.10 Configuration of figure 5.9 with closed inlet.

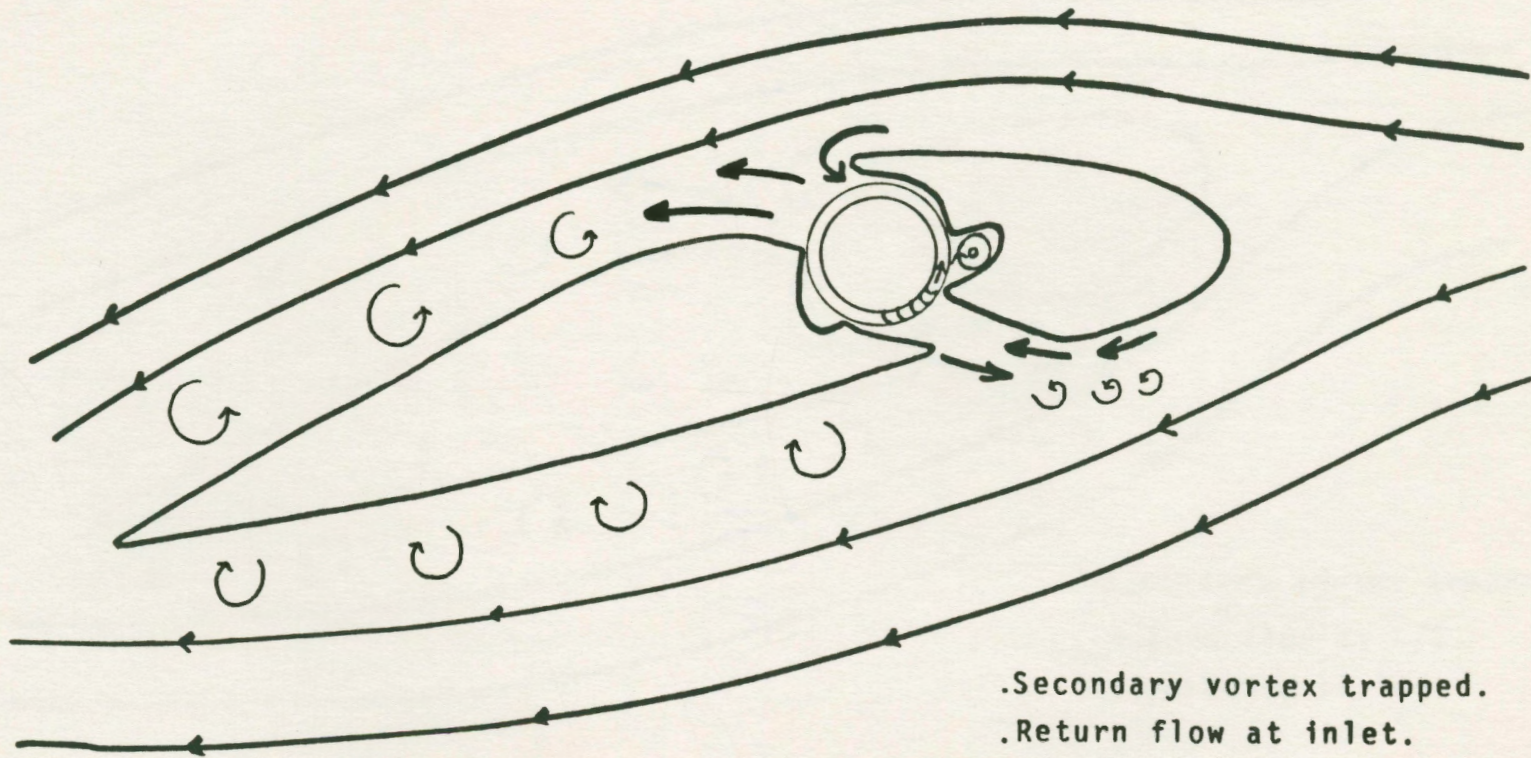
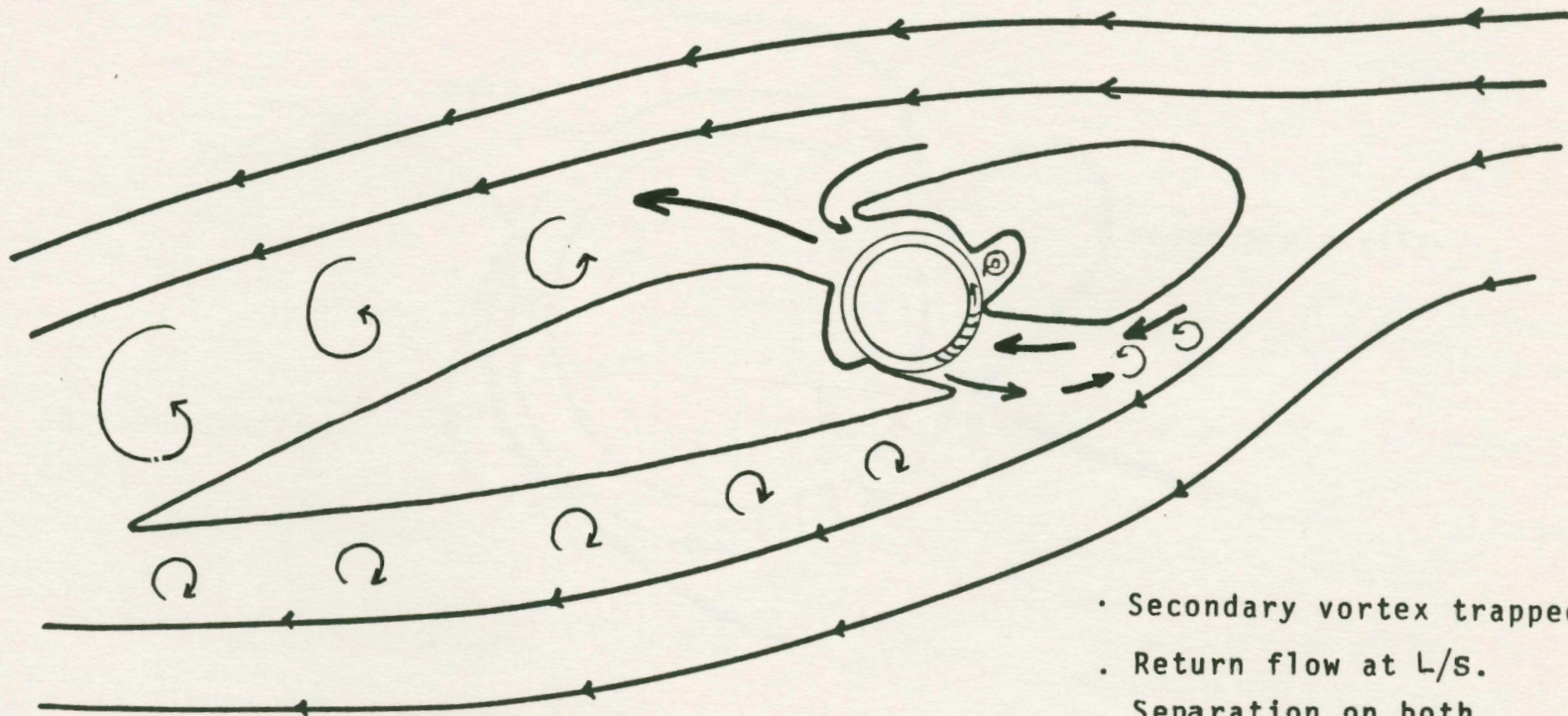


Figure 5.11 First airfoil at an angle of attack with dip nose.

- .Secondary vortex trapped.
- .Return flow at inlet.
- .Separation on both the U/S and L/S.
- .Suction from U/S leading edge.



- Secondary vortex trapped.
- Return flow at L/S.
- Separation on both surfaces.
- Suction from U/S leading edge.

Figure 5.12 First airfoil at angle of attack.

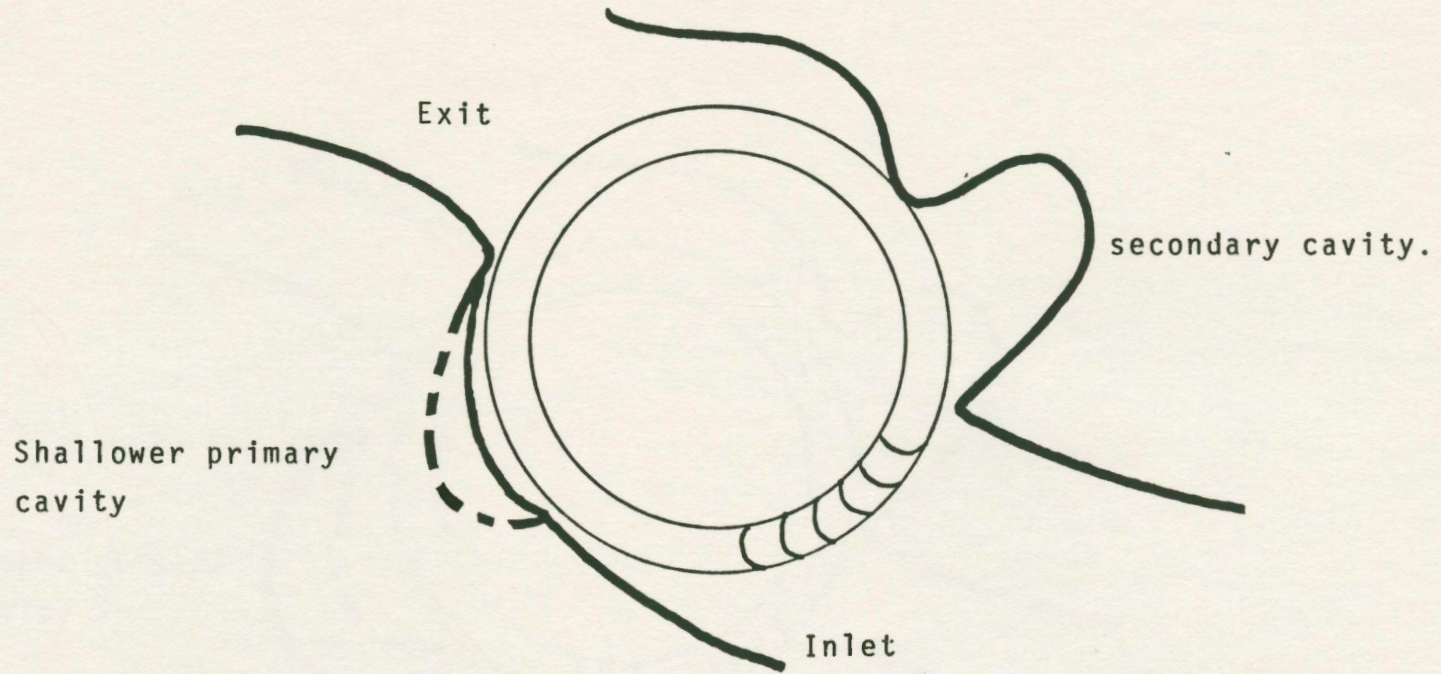


Figure 5.13 Second modification, shallower primary cavity.

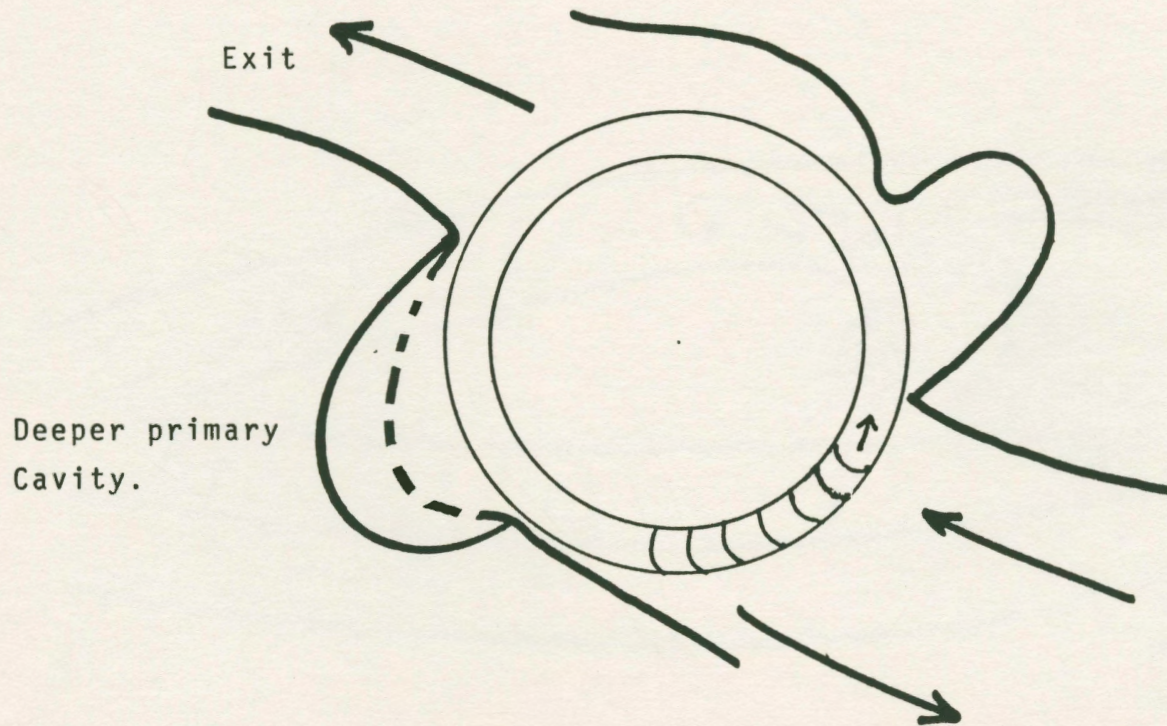
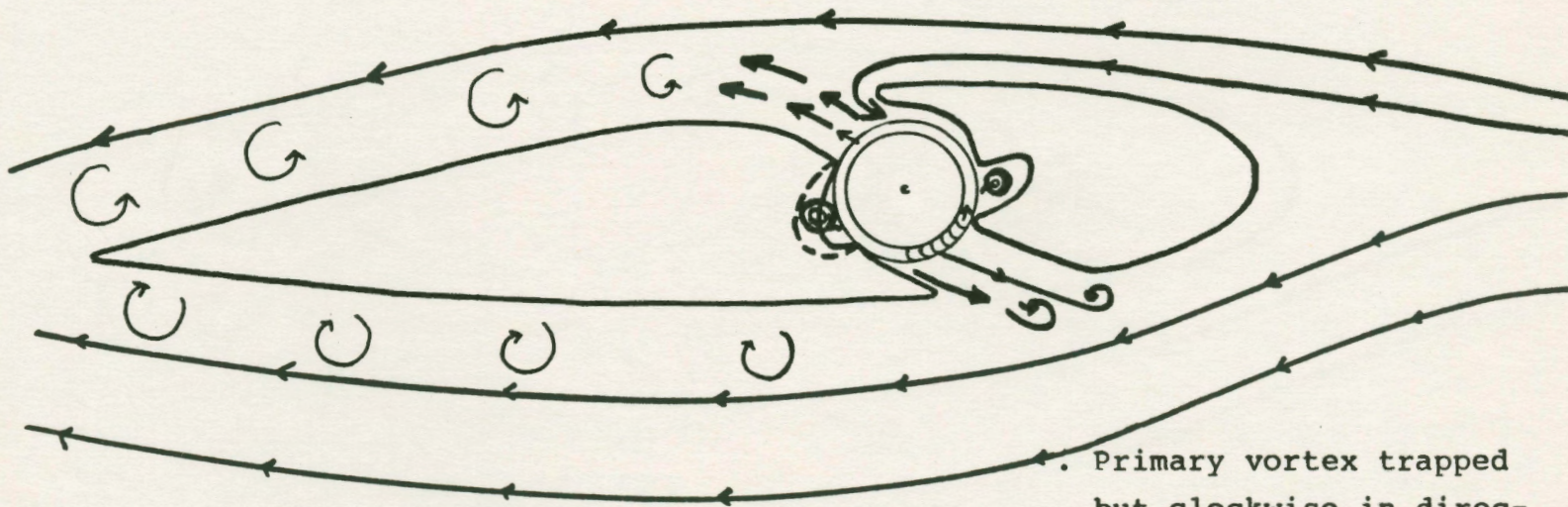


Figure 5.14 Third modification, deeper primary cavity.



- . Primary vortex trapped but clockwise in direction.
- . Suction from U/S leading edge.
- . Separation on U/S & L/S.

Figure 5.15 Deeper primary cavity in airfoil..

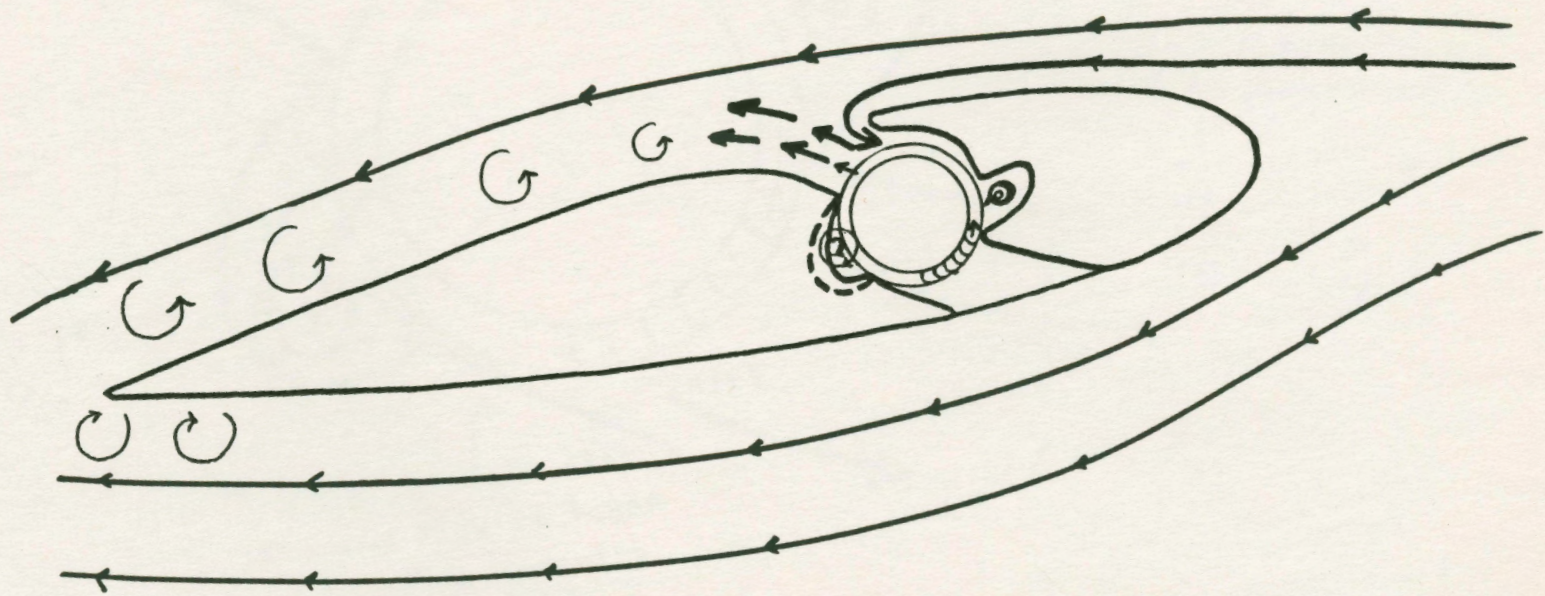


Figure 5.16 Configuration of figure 5.15 with closed inlet.

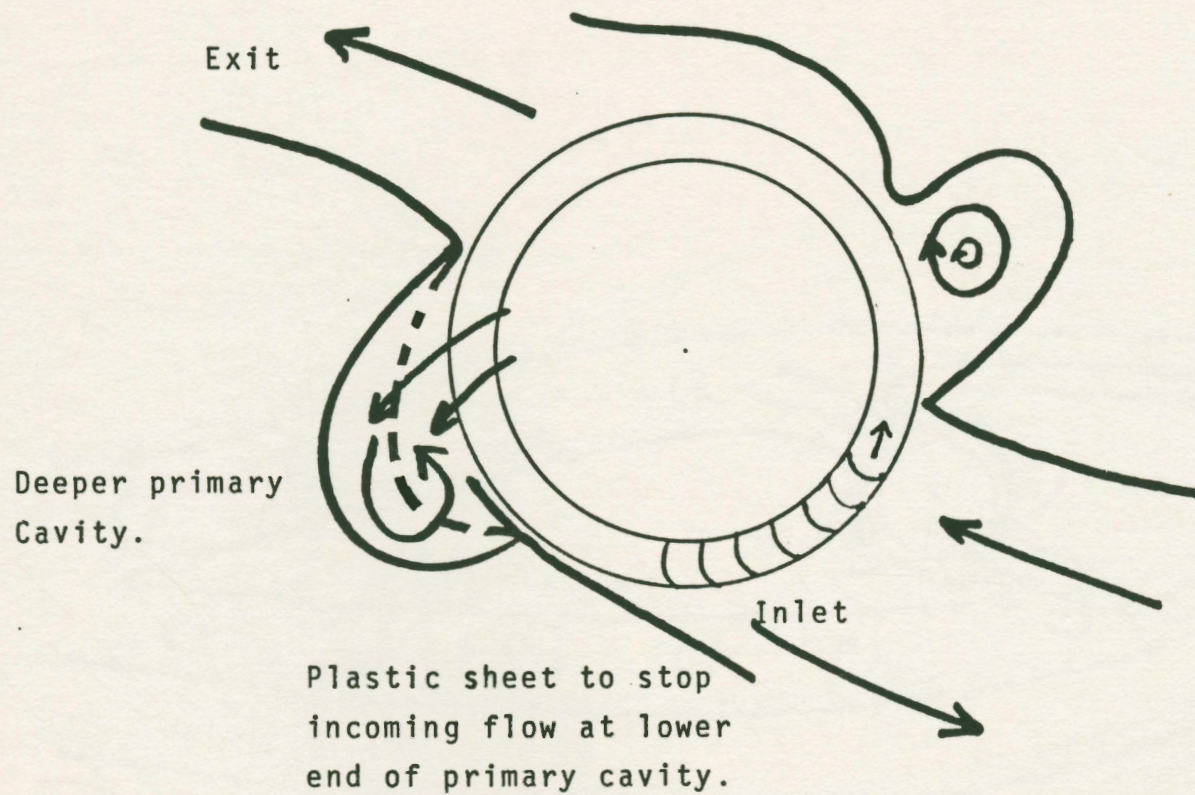
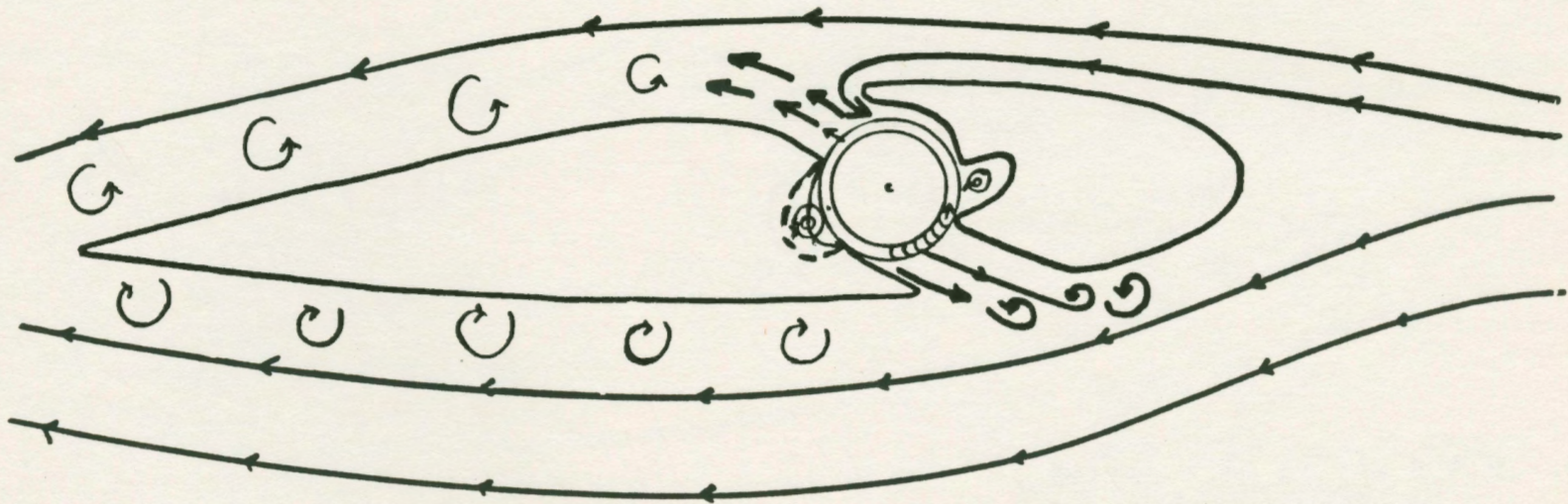


Figure 5.17 Forcing primary vortex to move in right direction.



- . Both vortices trapped.
- . Separation on U/S & L/S.
- . No suction from L/S.
- . Return flow at L/S.

Figure 5.18 Fourth modification, partial flow obstruction to primary cavity.

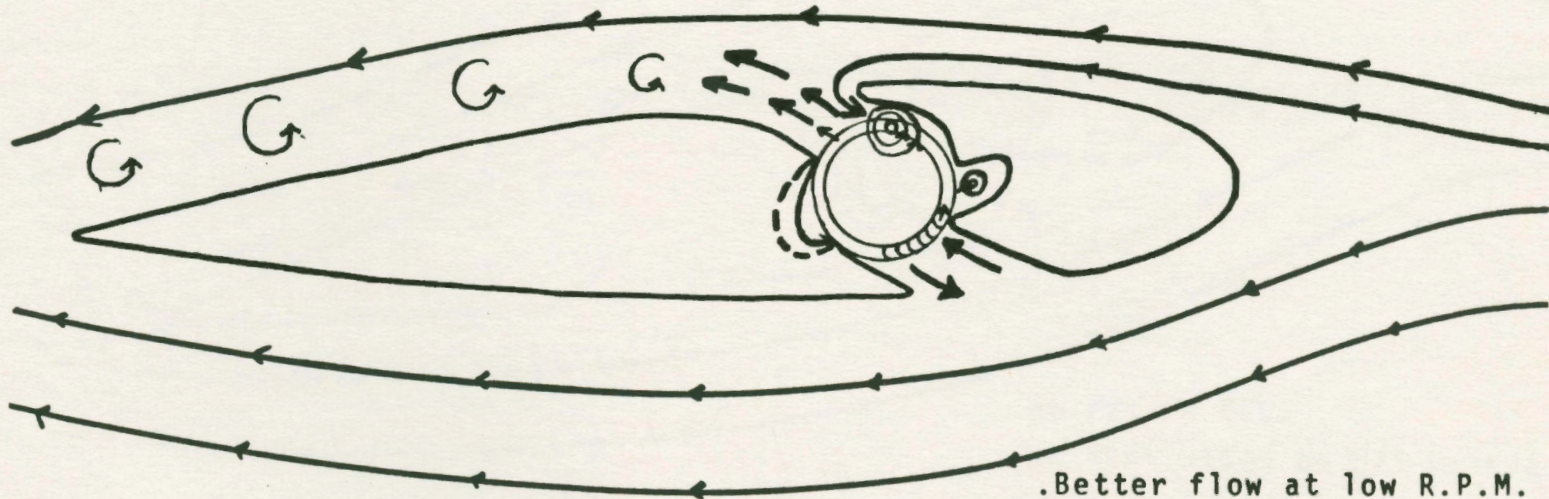
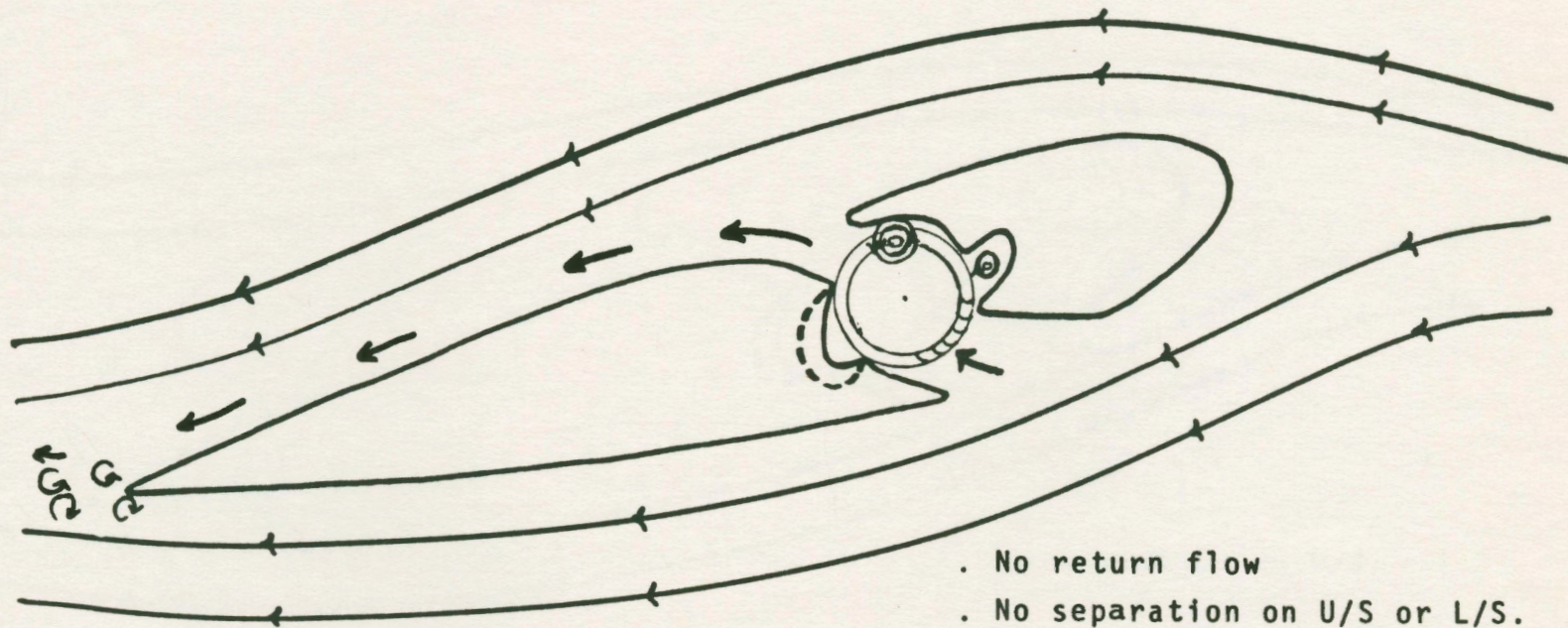


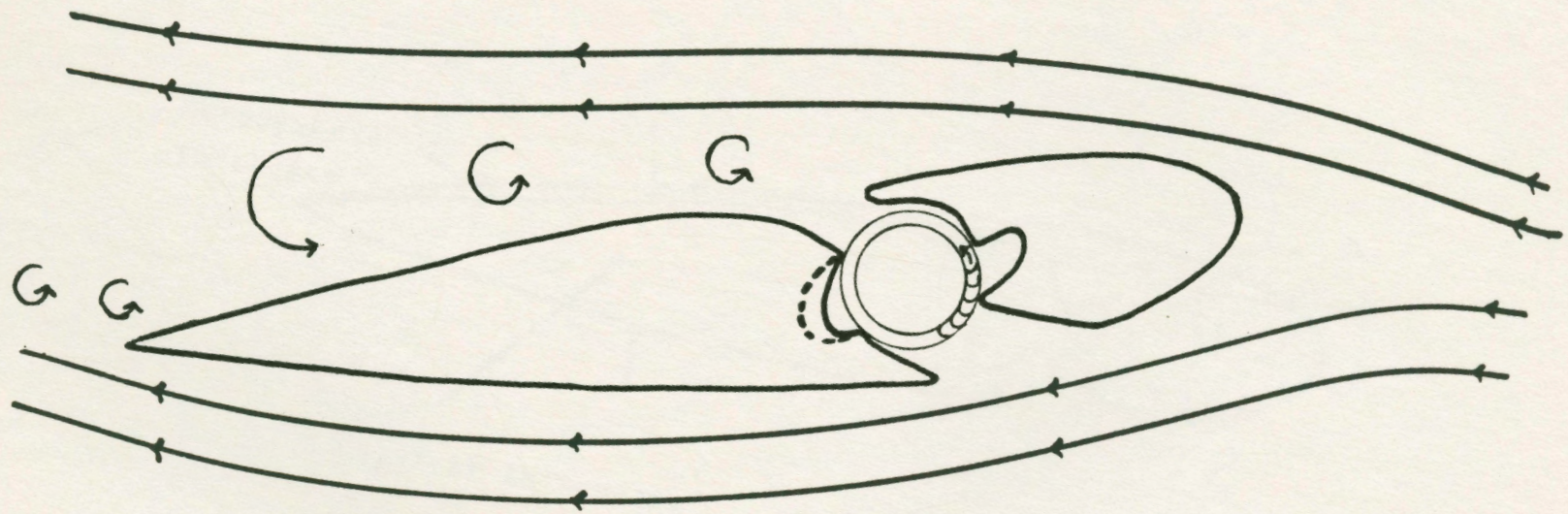
Figure 5.19 Low R.P.M Experiment.

- .Better flow at low R.P.M.
- .Suction from L/S also.
- .Return flow at L/S.
- .Separation on U/S.
- .Primary vortex center outside fan periphery.
- .Both vortices very weak.



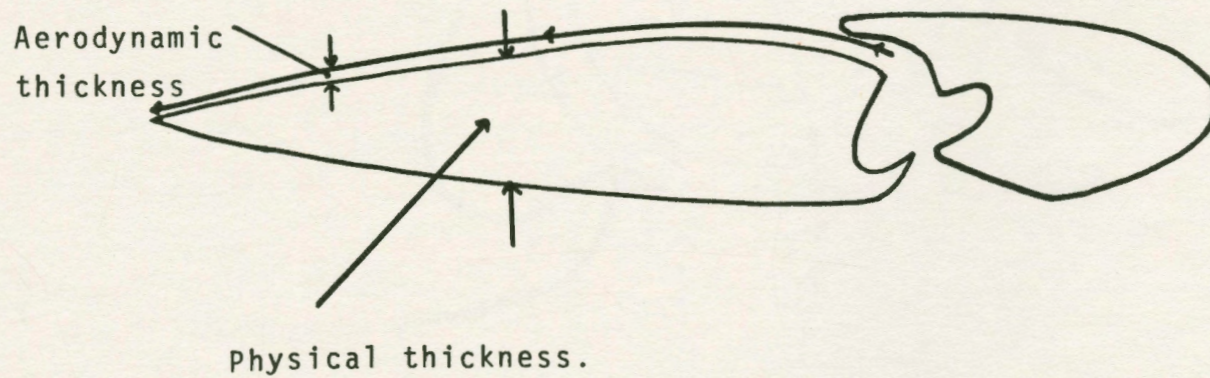
- . No return flow
- . No separation on U/S or L/S.
- . Both vortices trapped.

Figure 5.20 Low R.P.M experiment with airfoil at an angle of attack.
(Third Modification)



. Separation on U/S.

Figure 5.21 Configuration of figure 5.20 with fan off.



$$\text{Original thickness} = \text{Physical thickness} + \text{Aerodynamic thickness.}$$

Figure 5.22 Modified inlet and chord.

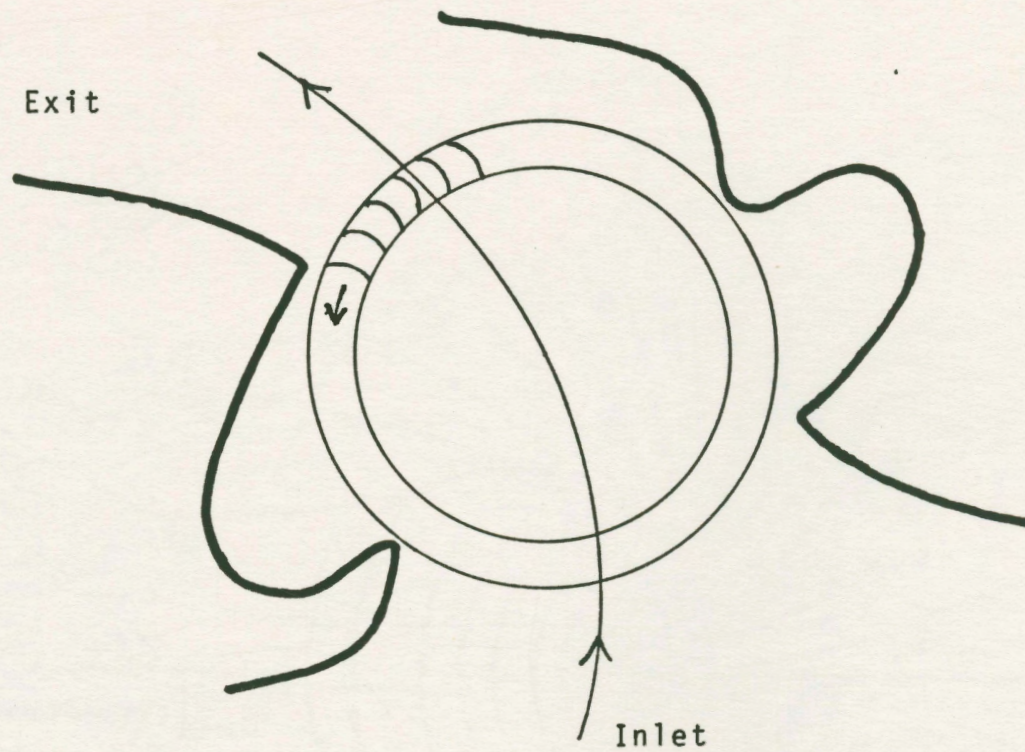


Figure 5.23 Modified Inlet with rear airfoil shaped so that flow can be Picked up from rear also.

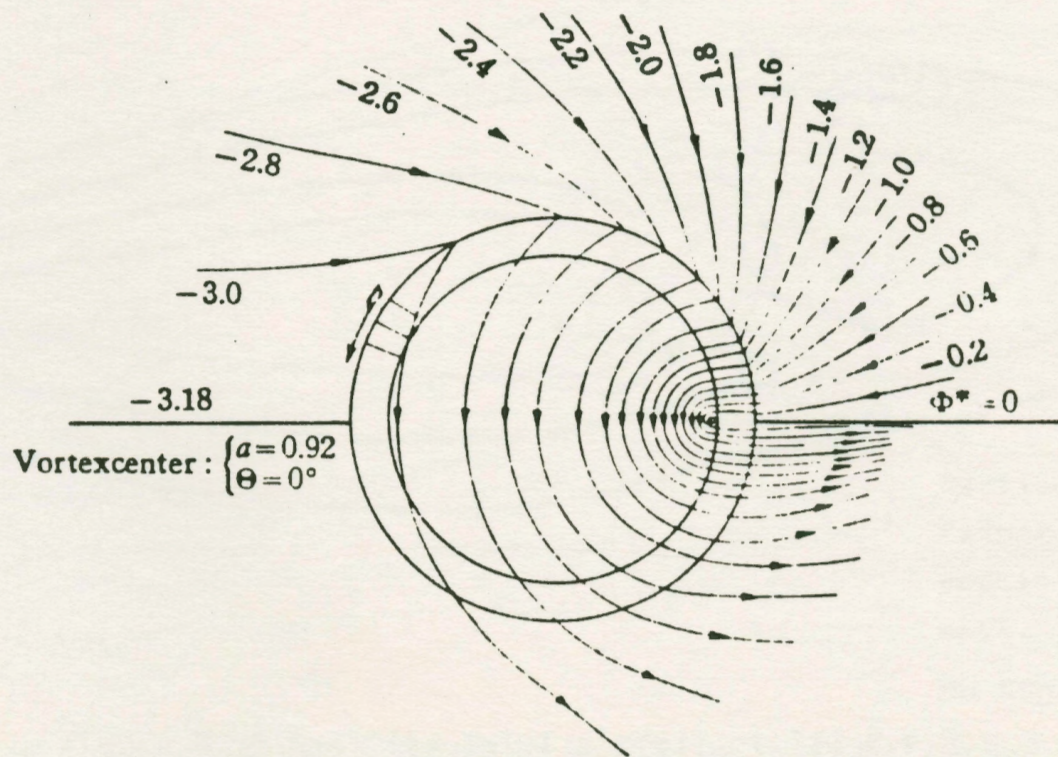
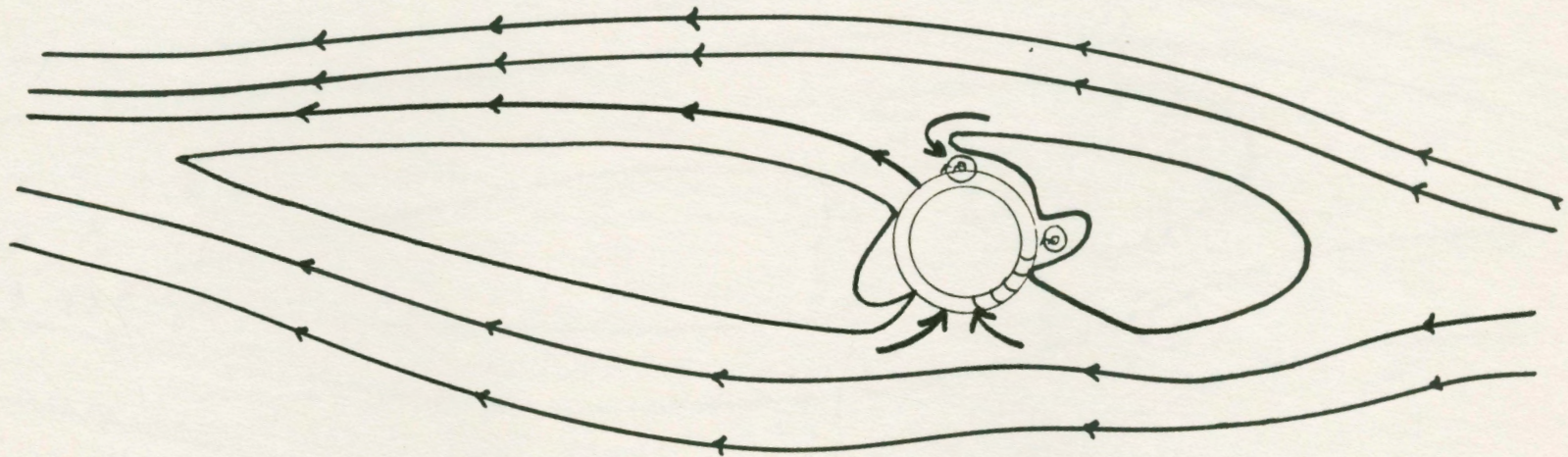


Figure 5.24 Theoretical streamline pattern through a C.F.F. (Ref 9)



- . Suction from U/S.
- . Primary and secondary vortices trapped but weak.
- . No Separation.

Figure 5.25 Modified Inlet airfoil at low R.P.M

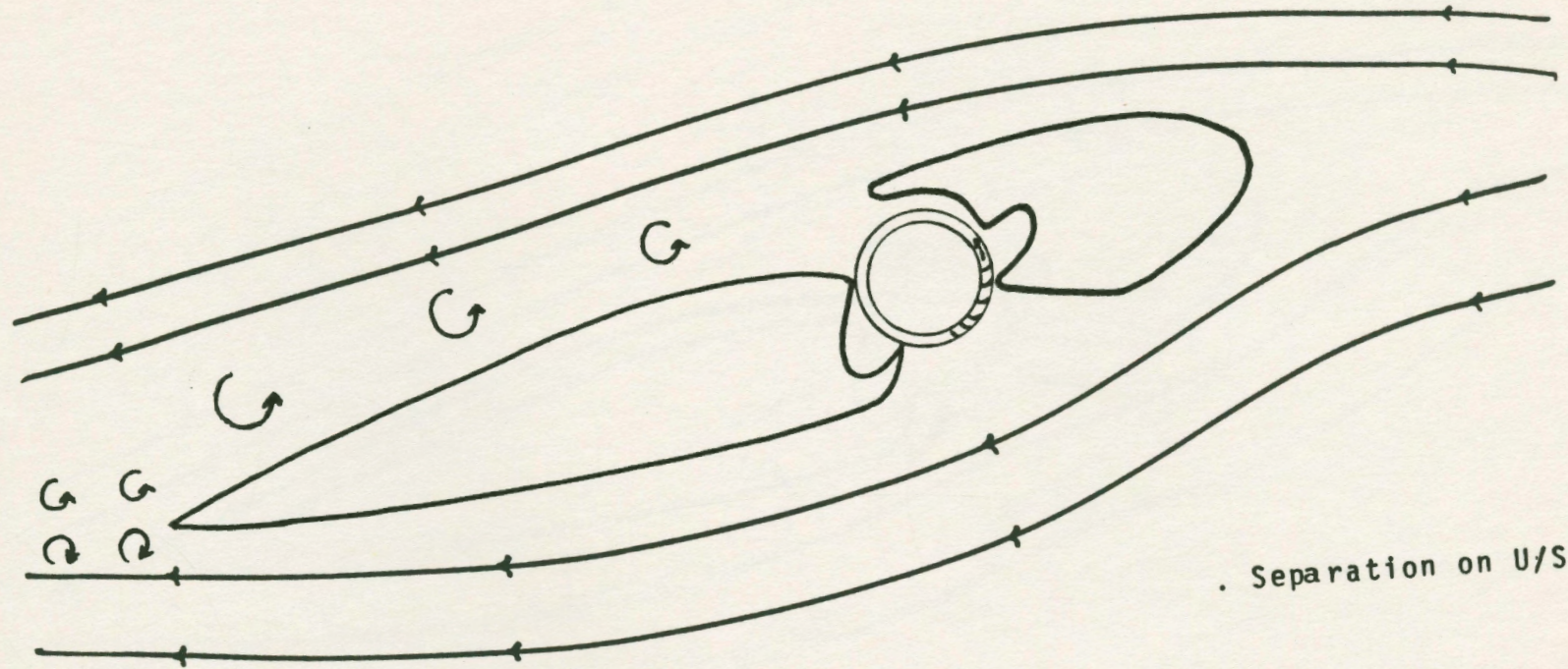
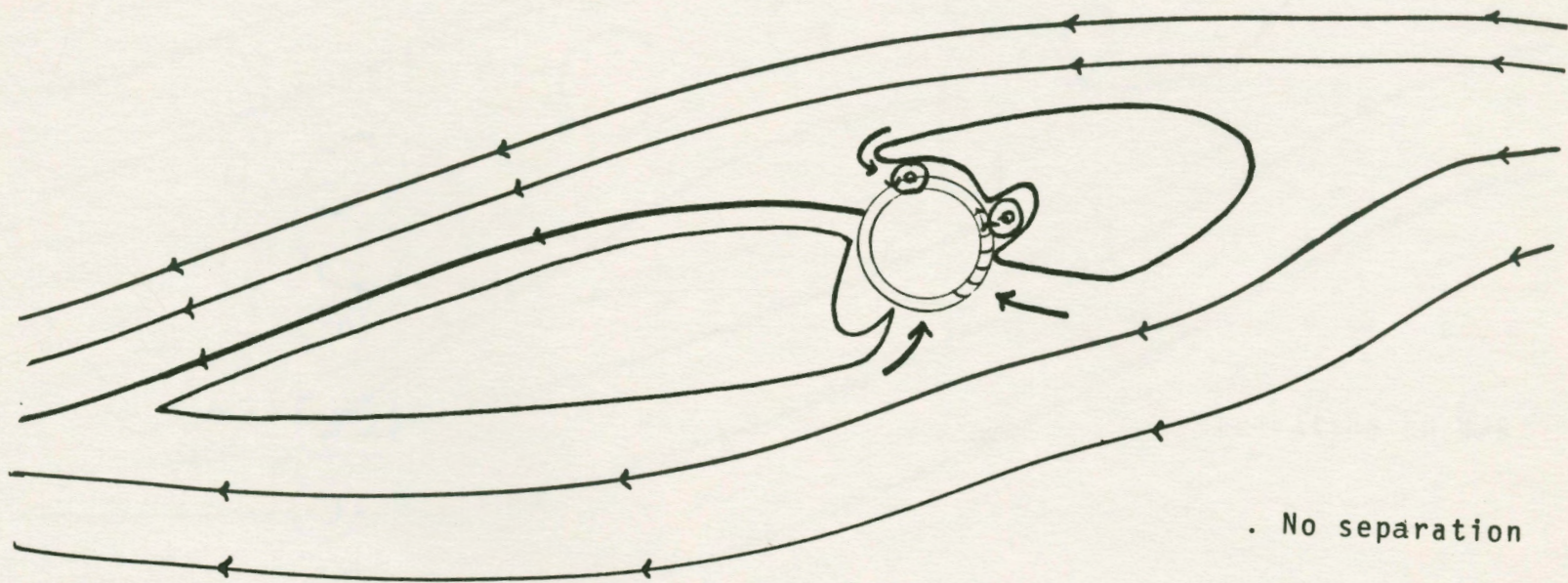


Figure 5.26 Modified inlet airfoil with fan off at low A.O.A.



. No separation

Figure 5.27 Configuration of figure 5.26 with fan running.

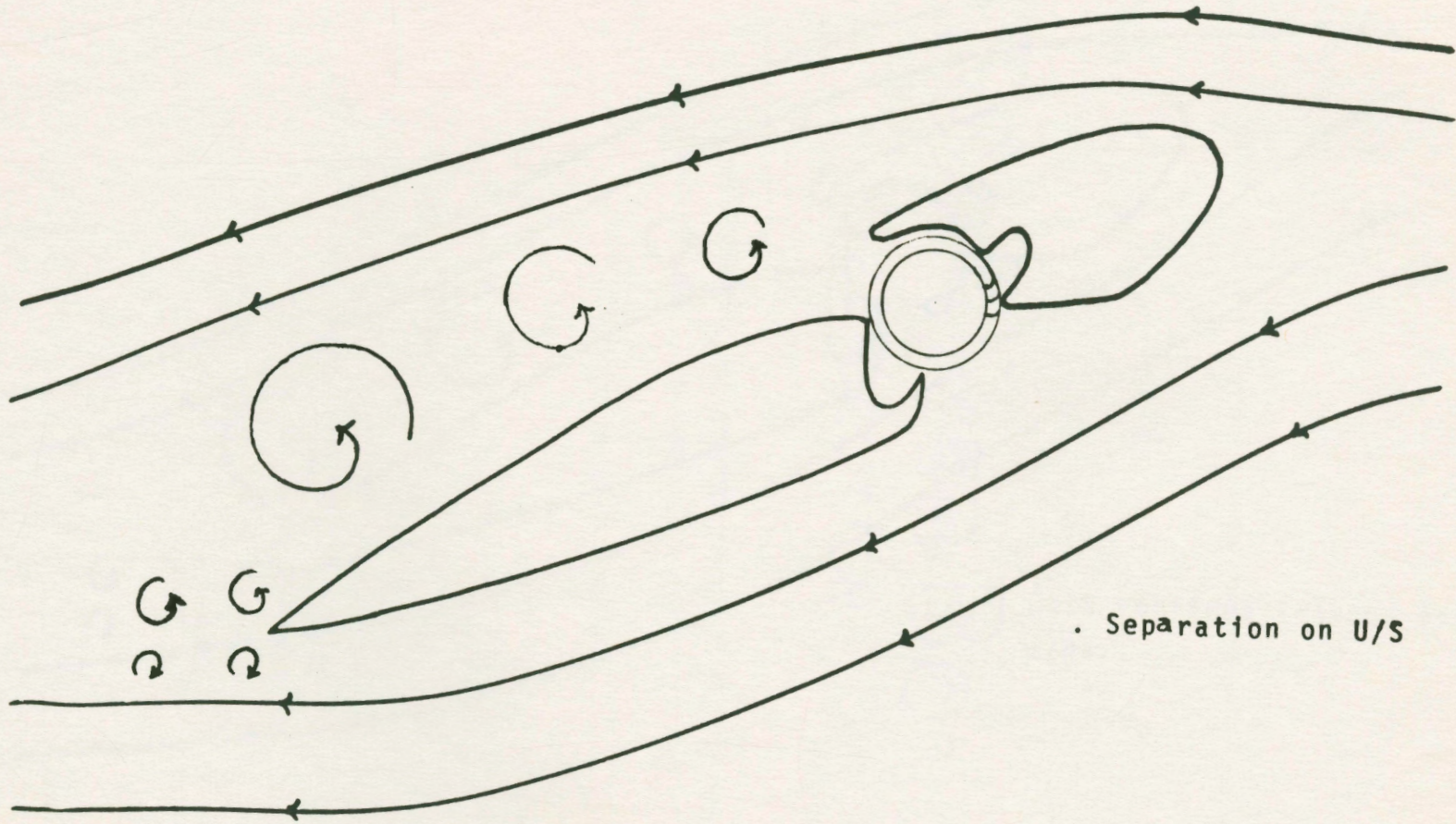
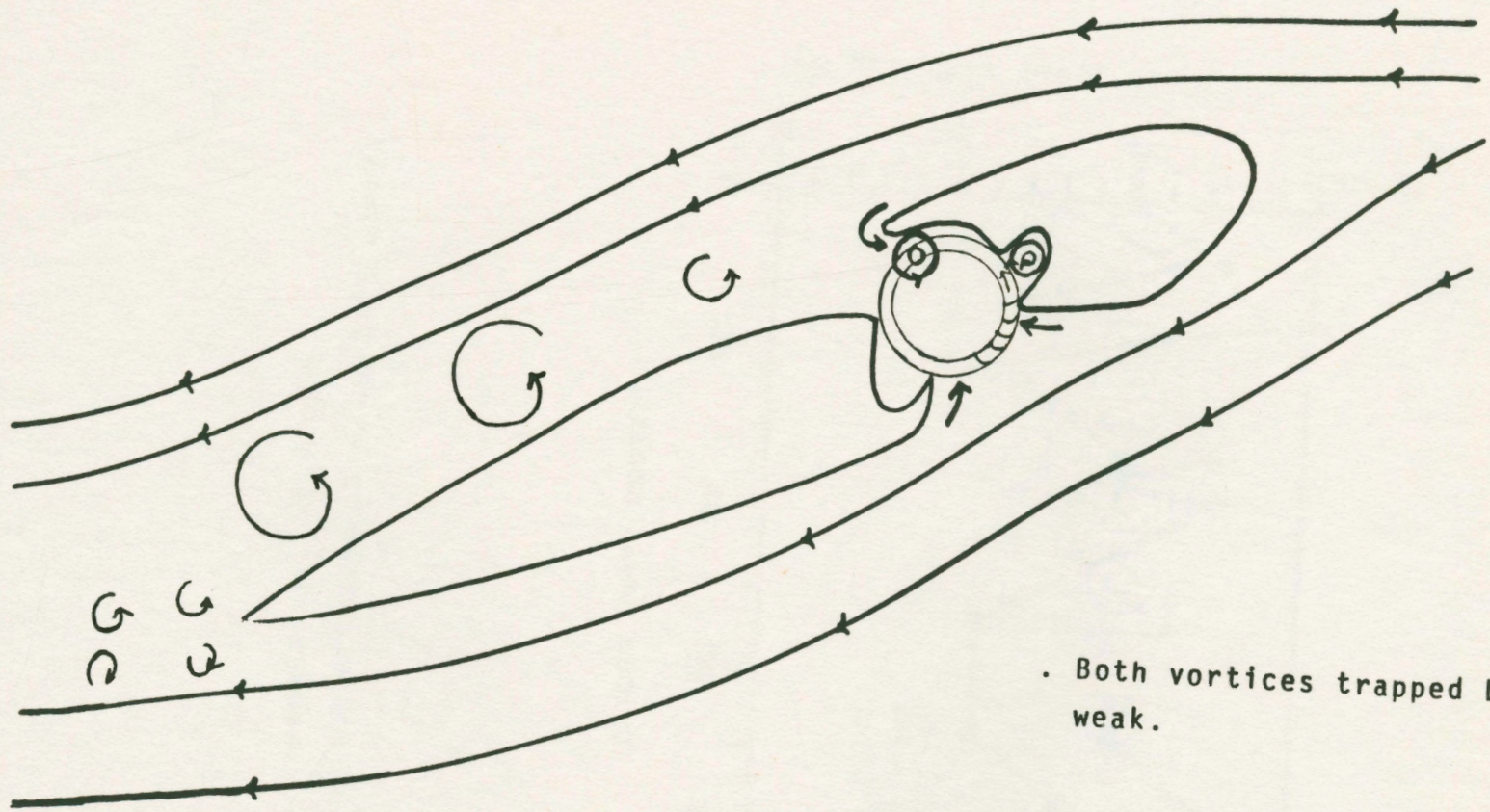


Figure 5.28 Modified inlet with fan off at High A.O.A.



. Both vortices trapped but weak.

Figure 5.29 Configuration of figure 5.28 with fan running.

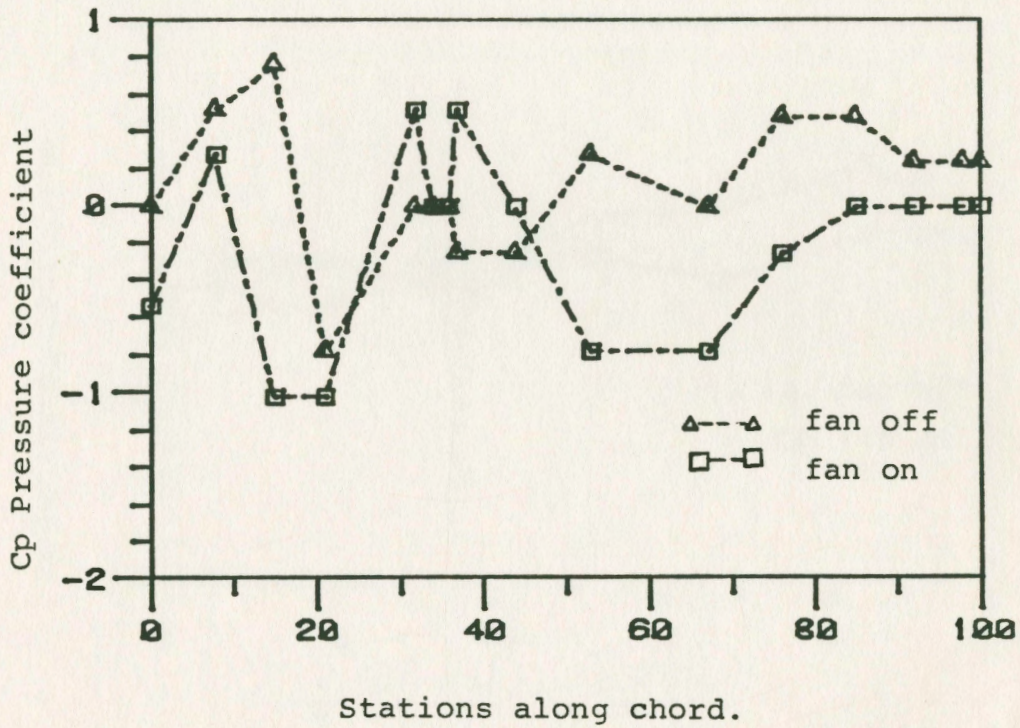


Figure 5.30 Pressure distribution on U/S along chord at $\alpha=12$ degrees.

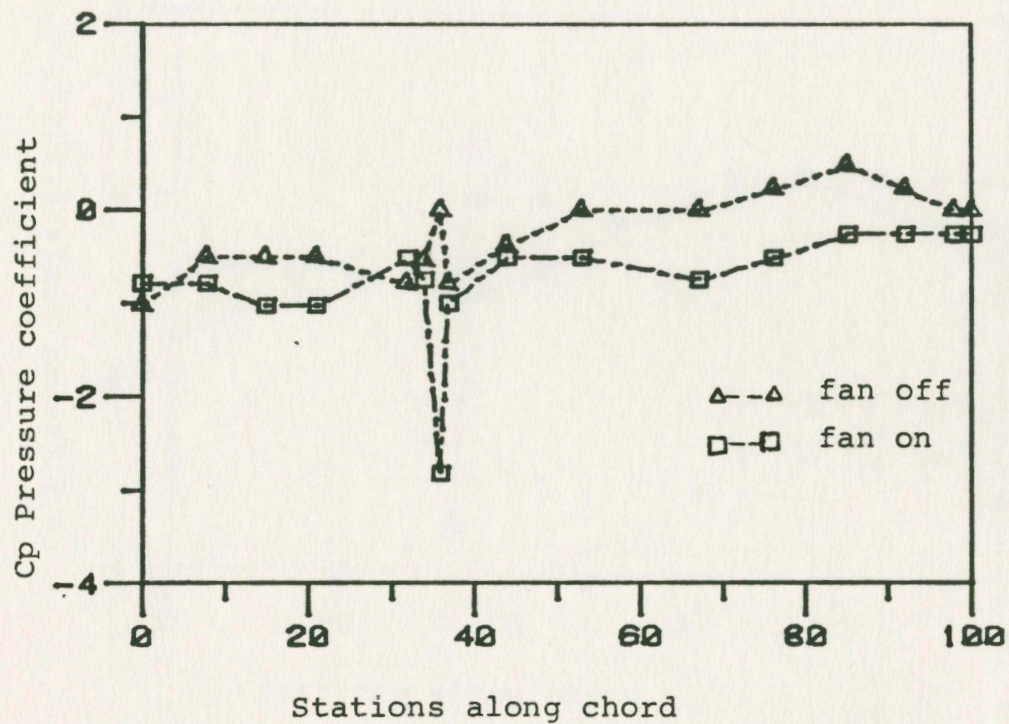


Figure 5.31 Pressure distribution on U/S along chord at $\alpha = 13.6$ degrees.

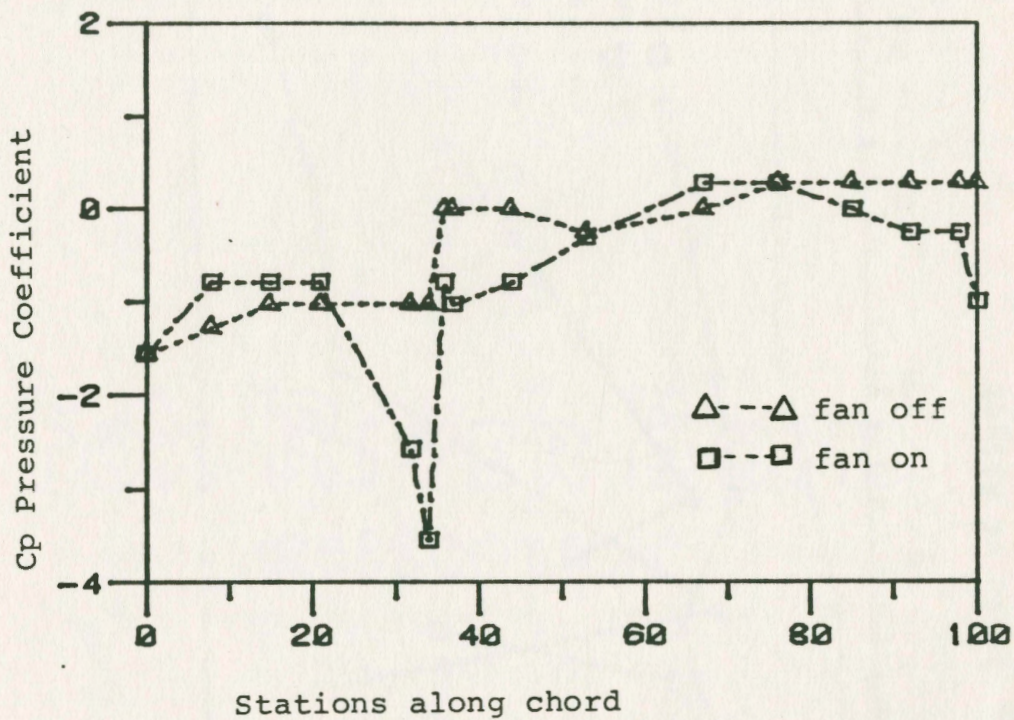


Figure 5.32 Pressure distribution on U/S along chord at $\alpha = 27$ degrees.

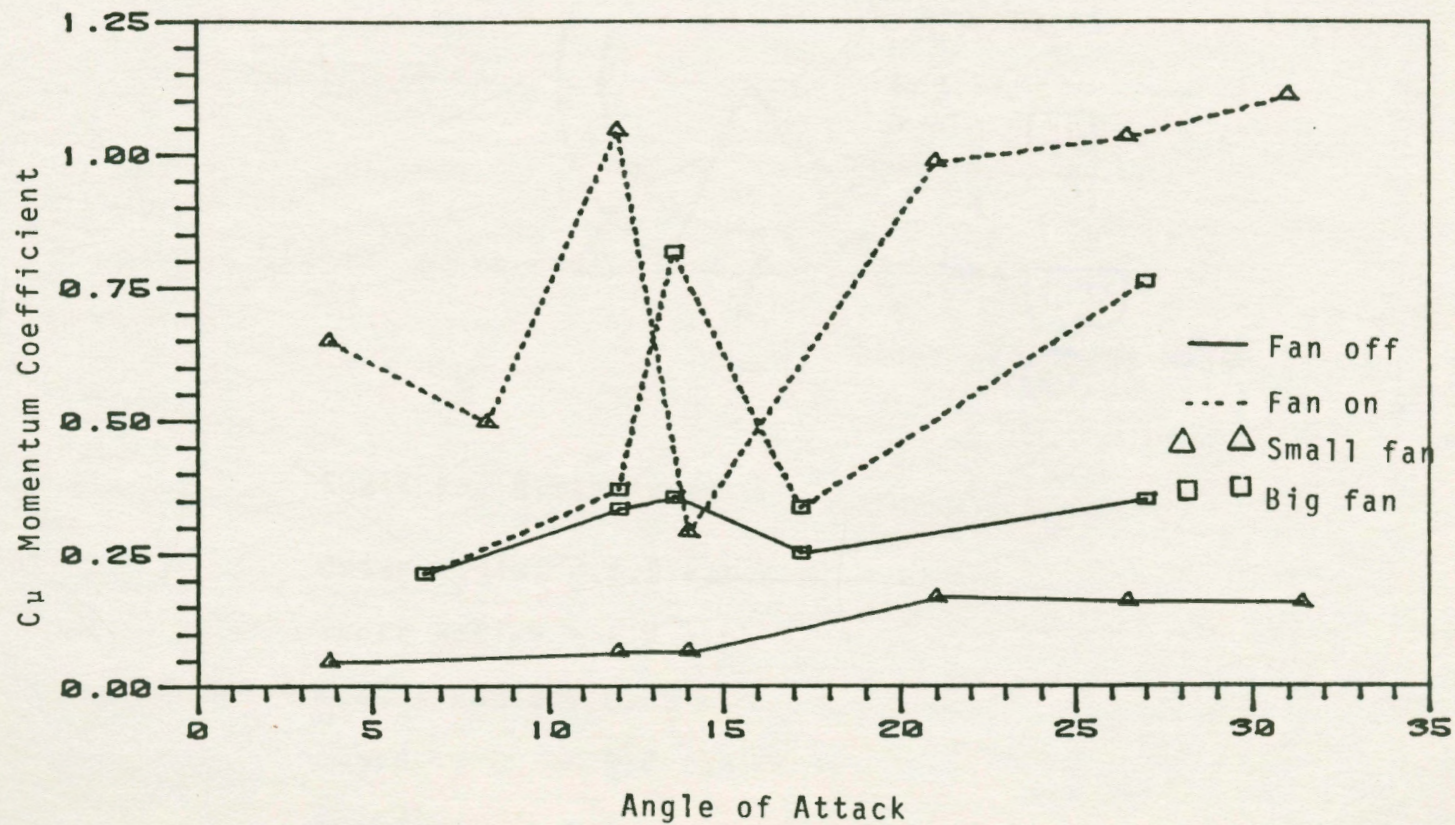
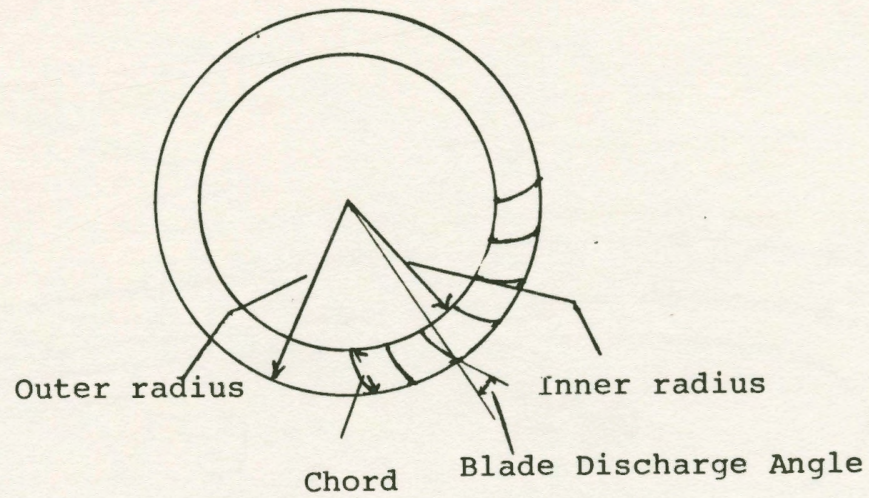


Figure 5.33 Momentum coefficient as a function of angle of attack.



Small Fan Dimensions:

Outer Radius = 2.5 c.m.

Inner Radius = 1.9 c.m.

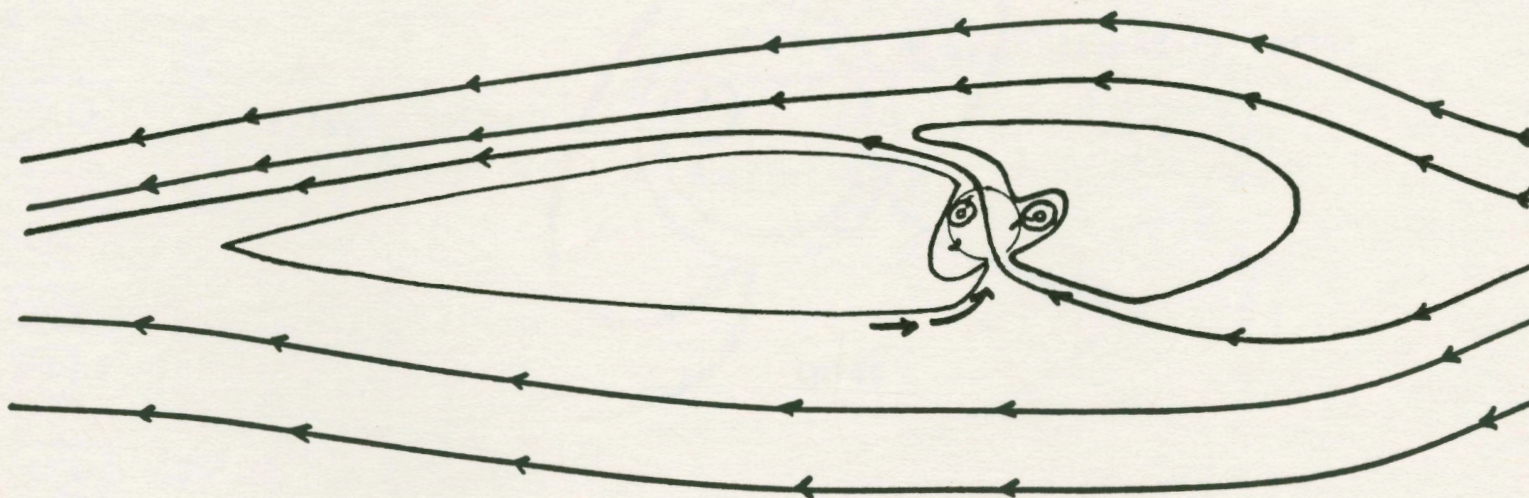
Radius Ratio = 0.76

Chord = 0.6 c.m.

Solidity = 1

Blade Discharge angle = 45°

Figure 5.34 Small Fan Dimensions.



- . Both vortices trapped.
- . Suction from L/S.
- . Good through flow.

Figure 5.35 Small fan experiment in the setup of modified inlet.

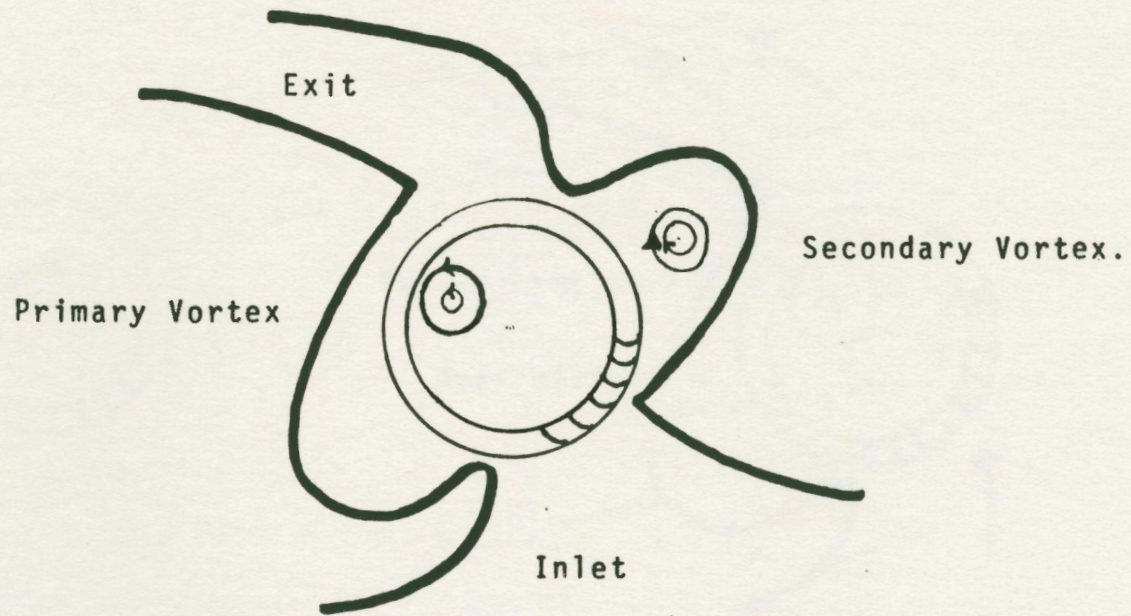
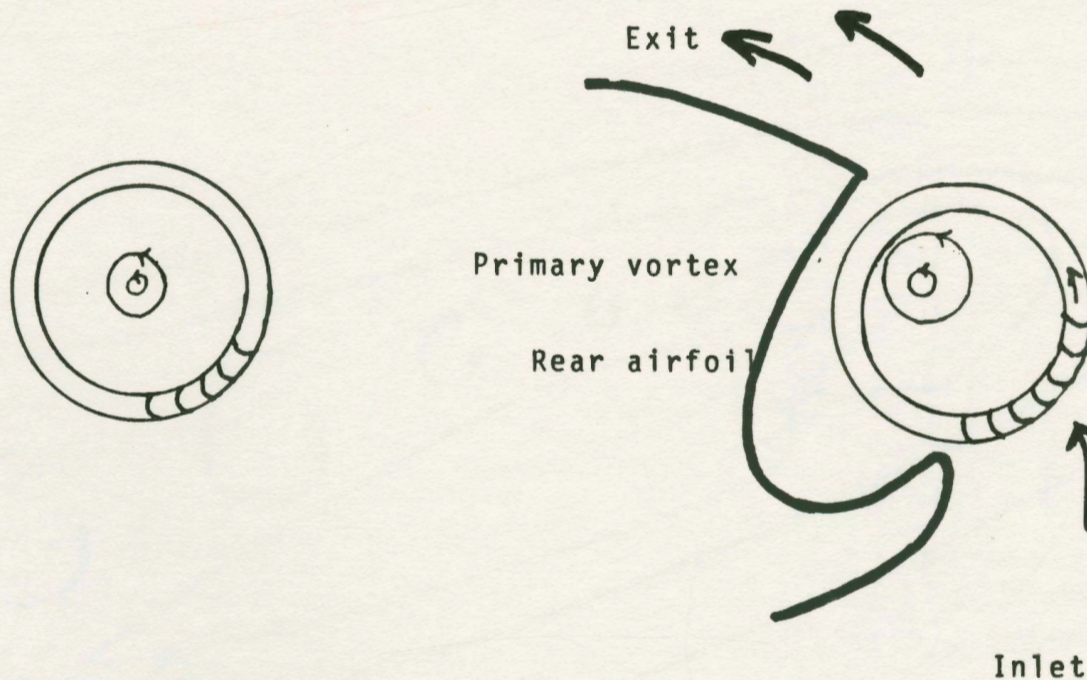


Figure 5.36 Location of centers of Primary and Secondary Vortices.



. Fan running without casing.
 . Vortex center near shaft center.

. Fan running with rear airfoil.
 . Vortex stabilised at a position away from center but inside the fan periphery.

Figure 5.37 Vortex location with and without casing.

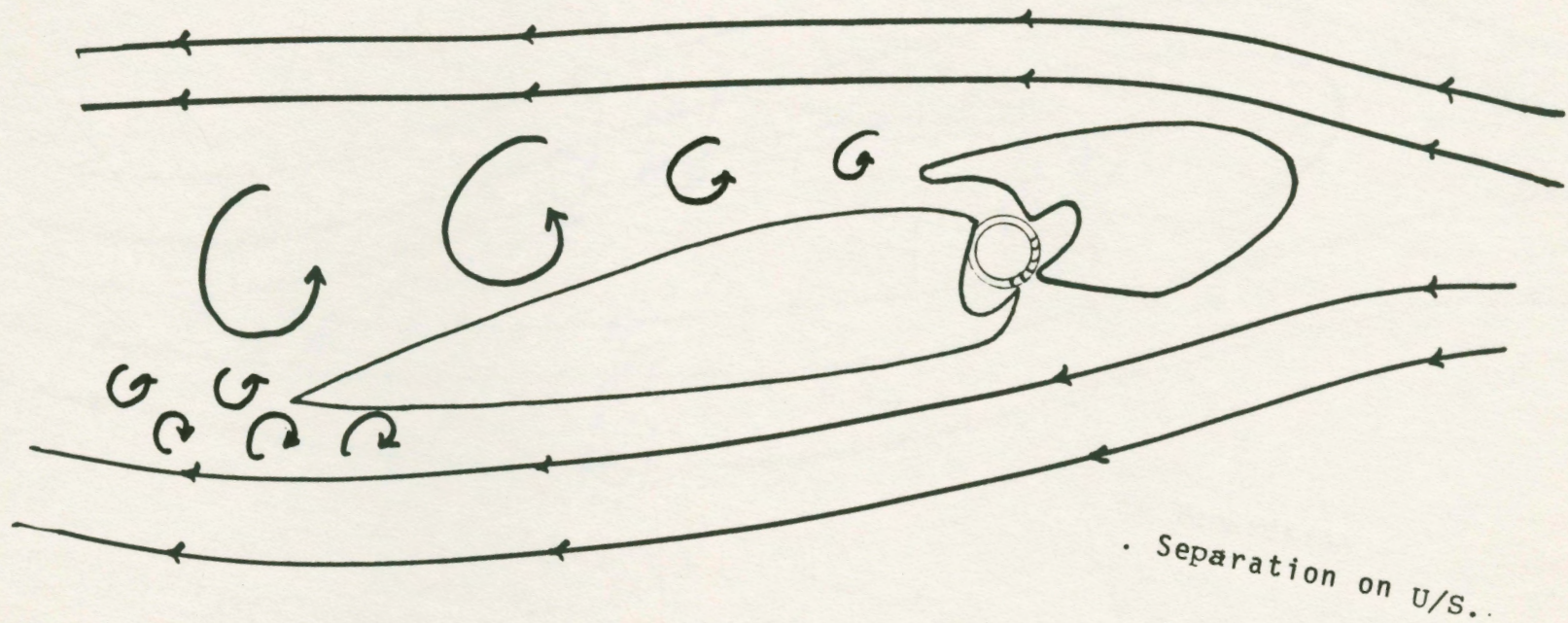


Figure 5.38 Airfoil with modified inlet and small fan at A.O.A.
 (Fan off.)

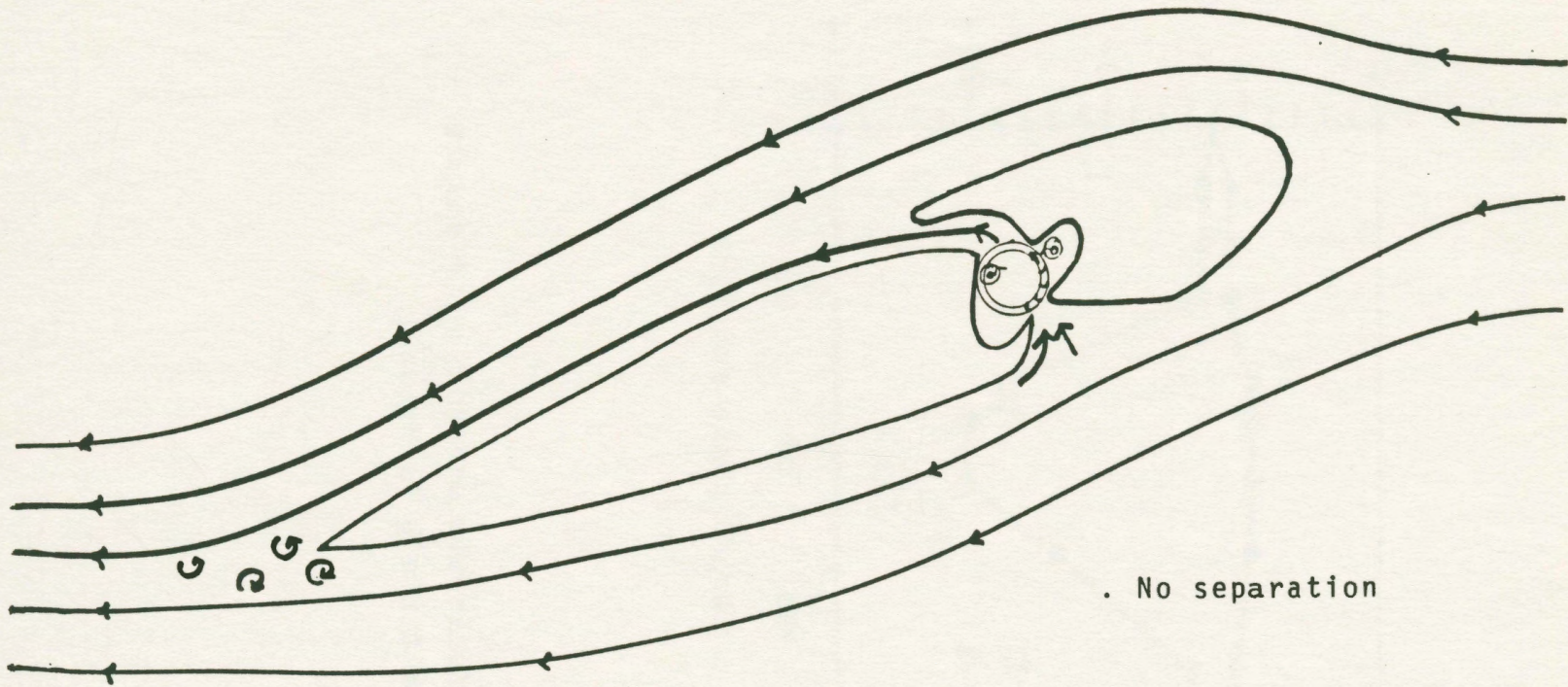


Figure 5.39 Configuration of figure with fan running.

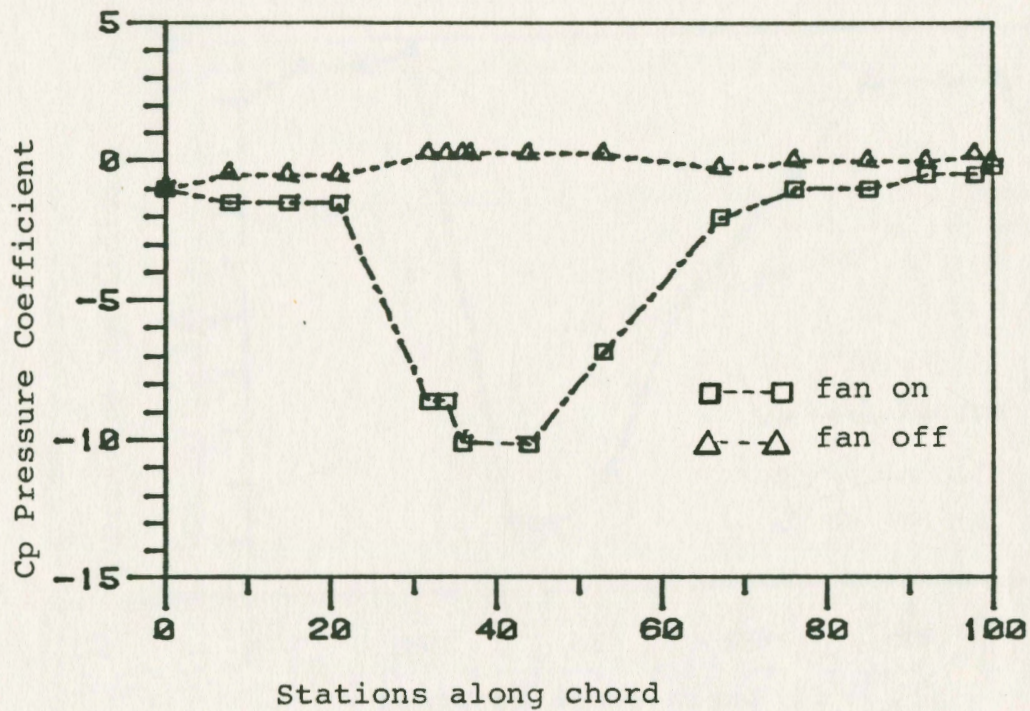


Figure 5.40 Pressure distribution on U/S along chord at $\alpha = 3.8$ degrees.

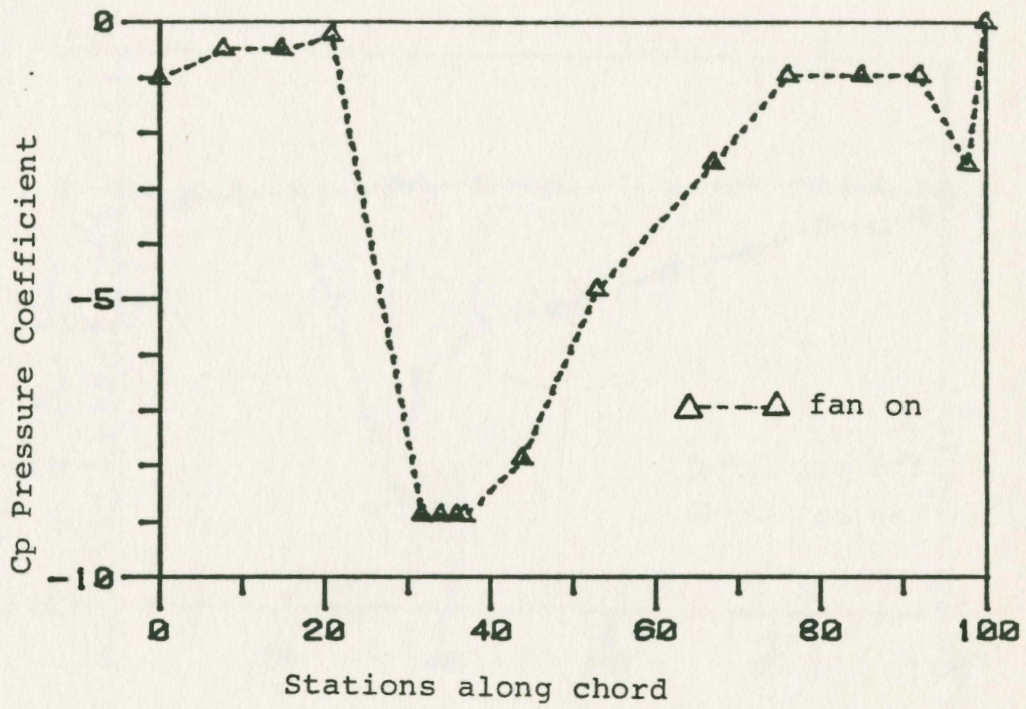


Figure 5.41 Pressure distribution on U/S along chord at $\alpha = 8.3$ degrees.

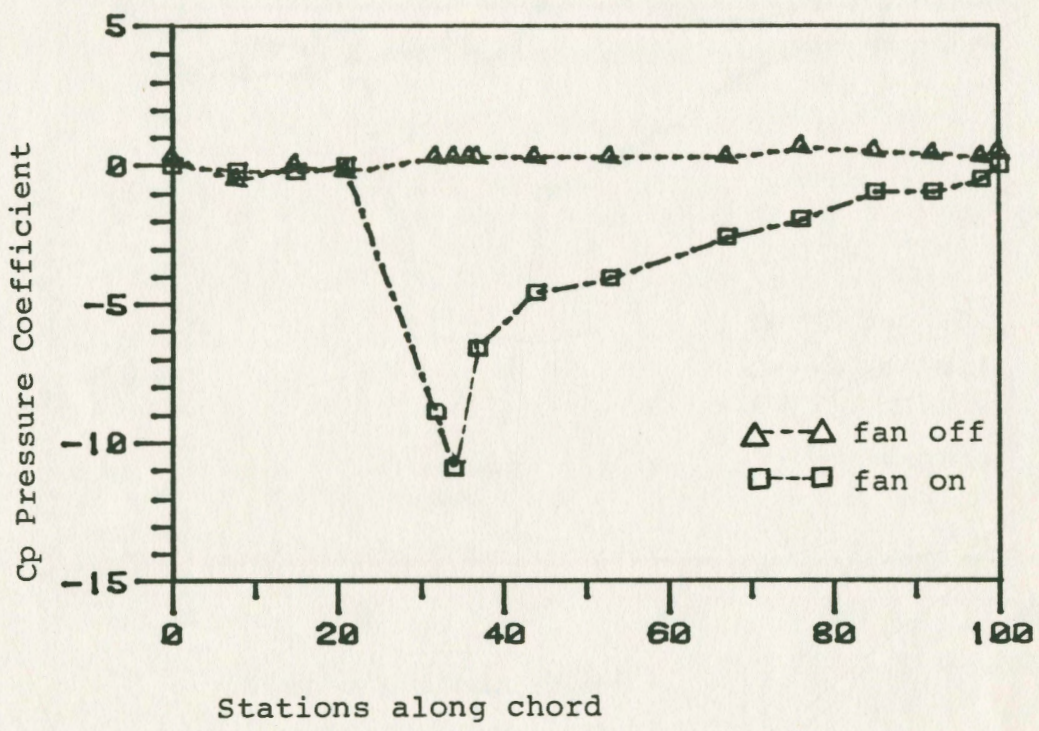


Figure 5.42 Pressure distribution on U/S along chord at $\alpha = 12$ degrees.

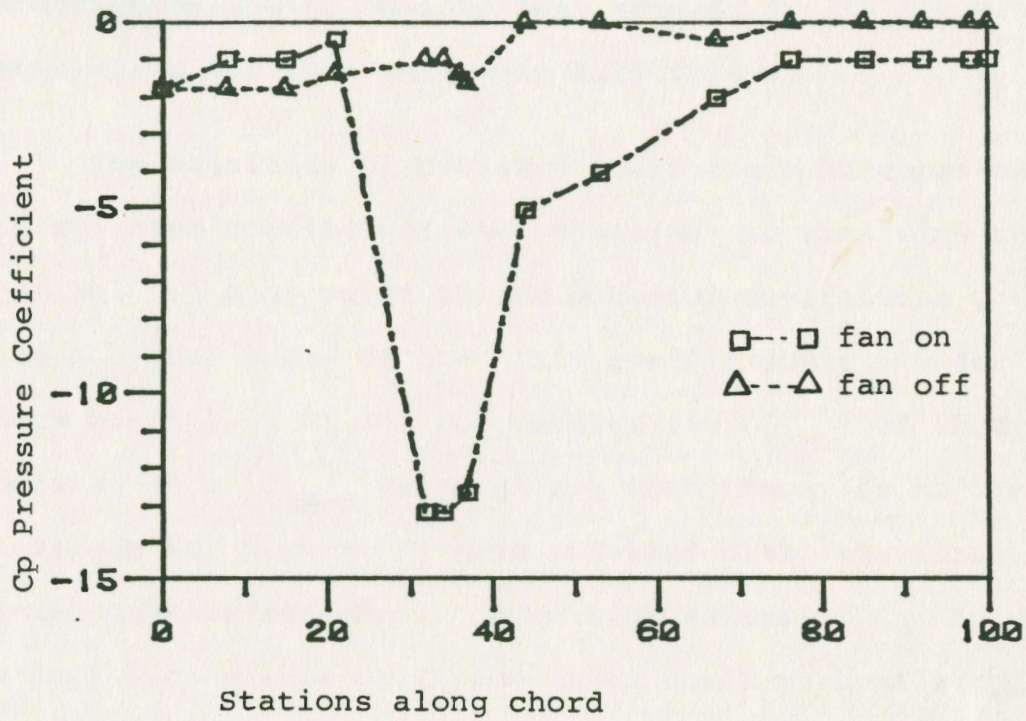


Figure 5.43 Pressure distribution on U/S along chord at $\alpha = 31.4$ degrees.

CONCLUSION

The final set up with modified inlet and reduced chord performed best with smaller fan running at 150 R.P.M. The water speed for this setup was 1.15 ft/sec.

The magnitude of pressure coefficient on upper surface and momentum coefficient were observed to rise with the fan running. A high value of the momentum coefficient C_μ would give a higher value of the lift coefficient C_l . For a 17% thick airfoil, C_μ of 0.4 results in C_{lmax} of about 5.5 compared to a C_{lmax} value of 1.2 when there is no blowing. C_μ values as high as 1 were obtained with the final setup of the present research. Such high values of C_μ could lead to very high values of C_l and thus could give an airplane a very impressive STOL capability.

Dimensional analysis of the first fan did not relate well to Harloff's fan (ref. 1). One possible reason could be that dimensional analysis does not include the effects of the housing shape. From the literature survey and based on the present research, it can be said that the housing shape is critical for the fan performance. The same fan, if installed in a bad housing, could very well result into very low values of the flow and pressure coefficients. Also the fan inlet and the outlet in the present research interact with the surrounding air, however there is no such

interaction in Harloff's fan (ref. 1). If in the non-dimensional velocity term (sec. 4.5), 'V' is the free stream velocity at infinity, then for Harloff's fan this coefficient had a value of zero, whereas in present research it has a finite value. Also proper geometric scaling of the fan involved in present research could not be obtained, as compared to Harloff's fan because of the manufacturing problems involved. Discharge angle for the fan in present research is very different from Harloff's fan.

The airfoil performed well for a large range of angles of attack with both the vortices trapped. The vortex center for primary vortex lied inside the fan periphery whereas the secondary vortex was captured in the high pressure cavity. Inlet, fan diameter, low pressure cavity design, R.P.M and outlet were observed to affect the fan performance considerably.

In the future, this final setup should be tested in the wind tunnel. Data should be collected at various angles of attack for lift and momentum coefficients with the fan on and off. C_L values can be related to C_M values and an estimate of C_L values can be made which would give an airplane STOL capability if this system were installed. The power required to create high C_L values can be calculated thereby assessing the practicality of installing a C.F.F. in an airplane.

REFERENCES

1. Harloff, G.J., "Cross Flow Fan Experimental Development and Finite Element Modelling", Ph.D. Dissertation, The University of Texas at Arlington, 1979.
2. Porter A.M. and Markland E., "A Study of the Cross Flow Fan", Journal Mechanical Engineering Science, Volume 12, No. 6, 1970.
3. Ilberg H. and Sadeh W.E., "Flow Theory and Performance of Tangential Fans", Proceedings of the Institution of Mechanical Engineers, Volume 180, Part 1, No. 19, 1965-66.
4. Hancock J.P., "Test of a High Efficiency Transverse Fan", AIAA Paper No. 80-1243, June 30, 1980.
5. Ibrahim Shukry K., "Design and Instrumentation of a Water Flow Channel and Application to some Aerodynamic Problems", Technical Documentation Report No. RTD-TDR-63-4024, 1963.
6. Anon., "Tangential Fan Design", Engineering Materials and Design, October 1965.
8. Hill Philip G. and Patterson Carl R., "Mechanics and Thermodynamics of Propulsion", 1965.
9. Ikegami Hiroshi and Murata Susumu, "A Study of Cross Flow Fan", Osaka University Technical Report, Volume 16, October 1966.

10. White Frank M., "Fluid Mechanics", Mc Graw Hill Company, NewYork, 1979.
11. Wenhan Su, Mouji Liu, Bocheng Zhou, Chenghao Qiu, Shanwen Xiong, "An Experimental Investigation of Leading Edge Spanwise Blowing", ICAS Report No. 82-662, 1982.
12. Harris M.J., Nichols J.H., Englar R.J. and Huson G.G., "Development of the Circulation Control Wing / Upper Surface Blowing, Powered Lift System for STOL Aircraft", ICAS Report No. 82-651, 1982.

- 10. White Frank M., "Fluid Mechanics", Mc Graw Hill Company, New York, 1979.
- 11. Wenhan Su, Mouji Liu, Bocheng Zhou, Chenghao Qiu, Shanwen Xiong, "An Experimental Investigation of Leading Edge Spanwise Blowing", ICAS Report No. 82-662, 1982.
- 12. Harris M.J., Nichols J.H., Englar R.J. and Hanson G.C., "Development of the Circulation Control Wing \ Upper Surface Blowing, Powered Lift System for STOL Aircraft", ICAS Report No. 82-651, 1982.

Original
4722